MICROFLUIDIC CHIP-BASED FABRICATION OF HOLLOW ALGINATE MICROFIBER FOR ENZYME ENTRAPMENT AND REACTION

by

UYEN HOANG THAO PHAM

Presented to the Faculty of the Graduate School of
The University of Texas at Arlington in Partial Fulfillment
of the Requirements
for the Degree of

MASTER OF SCIENCE IN BIOENGINEERING

THE UNIVERSITY OF TEXAS AT ARLINGTON

August 2013

Acknowledgements

I would like to express my profound appreciation to my professor and thesis mentor Dr. Samir M. Iqbal. During my four years as an undergraduate and a graduate research student in the Nano-Bio Lab, his guidance and motivation has always meant a lot to me. As an advisor, he always offered me an opportunity to discuss research and my work freely and openly. His patience and encouragement is the reason for who I am today and made all of this work possible.

I would like to thank my committee members Dr. Kytai Nguyen and Dr. Young-Tae Kim for their time, support, and enthusiasm. I would also like to thank Dr. Amit Asthana, Dr. Purnendu (Sandy) Dasgupta, and Dr. Subhrangsu Mandal.

I would like to thank all of my colleagues at the Nano-Bio Laboratory. Their discussions and suggestions helped me tremendously. My sincere thanks to Jeyantt, Madiha, Cuong Le, Raziul Hasan, Arif, Sirisha, Loan Bui, and Jyothi for their support and encouragement.

I would like to dedicate this work to my family who always support me with their love and patience through all my endeavors.

July 15, 2013

Abstract

MICROFLUIDIC CHIP-BASED FABRICATION

OF HOLLOW ALGINATE MICROFIBER

FOR ENZYME ENTRAPMENT

AND REACTION

Uyen Hoang Thao Pham, MS

The University of Texas at Arlington, 2013

Supervising Professor: Samir M. Iqbal

This thesis demonstrates a simple process to generate alginate hollow microfibers by using a non-lithographic PDMS microfluidic device. The microfluidic device was fabricated by a novel template method in a wet lab without the support of any conventional lithography techniques. The relationships of the flow rate and the diameter of hollow alginate fibers were characterized. It was found that the outer diameter of the alginate hollow fiber was independent of the flow rate, but the core flow and sheath flow played an important role to control the internal diameter and the wall thickness of the alginate hollow microfiber. At a constant sheath flow and at increasing core flow rates, the internal diameters increased and the wall thicknesses decreased. At a fixed core flow, with increasing sheath flow rates, the internal diameters decreased and the wall thicknesses increased. The fabricated alginate hollow microfiber was then used as a bioreactor. Glucose oxidase (GOx) was chosen as a model enzyme that was entrapped in the hollow microfibers. The GOx enzyme activity was investigated by a colorimetric assay. This showed that a small internal core and a thick wall directly affected the enzyme encapsulation efficiency, enzymatic activity, and enzyme leakage. In addition,

the metal ions present in an enzyme storage solution could act as activators or inhibitors changing the enzyme activity.

Table of Contents

List of Illustrations

Chapter 1

Introduction

An enzyme is a biocatalyst molecule that binds to its substrate, forming a complex and contains a specific activity. An enzyme catalyzes and increases the rate of a chemical reaction a million times faster than uncatalyzed reaction by lowering the activation energy. The benefits of enzymes have been applied in many different industrial and analytical processes. However, it is very difficult to handle the enzymes because of their sensitivity. In an unfavorable environment, enzymes become unstable, are easy to denature, or experience loss of enzymatic activity. In addition, the processes of isolation and purification are costly, low in efficiency, and are limited for long time storage. Therefore, it is very important to develop a technique to overcome these limitations.

Enzyme immobilization is a process in which enzyme is attached or held in a confined space or a substrate keeping it stable in unfavorable conditions. Techniques to immobilized enzymes have been developed continuously over many years. The most common immobilized methods are physical adsorption, covalent crosslinking, and entrapment. Physical adsorption is the simplest method that attaches immobilized enzyme via weak bonding. The disadvantage of this method is that weak bonding makes it easy to remove enzyme with change in surrounding media, ionic strength, or pH. Enzymes can also be immobilized via covalent crosslinking which forms a strong bond between enzymes and the functional group on the substrate material. However, this technique can alter enzyme conformation or even cause loss in enzymatic activity. Entrapment is a technique that cages enzymes in a confined space. The loss of enzymatic activity using this method is minimized because this technique does not affect the enzyme conformations. In this method, the leaching of enzyme from the substrate depends on the ratio between pore sizes of support material and the size of immobilized

biocatalyst molecules. Therefore, choosing support material is a critical factor in entrapment method.

Different microstructures are used for enzyme immobilization such as microbeads/microspheres, microstrips, or microfibers. Immobilized cells and various biocatalysts inside fiber microstructures have been developed at a rapid pace in recent years. Microfiber is fabricated as a responsive structure that can be used as an individual microscale sensing device or as a component in a microdevice [1]. Many different techniques can be used to generate microfibers such as electrospinning, wetspinning, interfacial complexation, meltspinning, and microfluidic channels. In all of these fiber-based techniques, a microfluidic device is considered to be a convenient method for cell or sensitive biocatalyst immobilization.

1.1 Objective

The aim of this thesis was to immobilize enzymes by entrapping them in an alginate hollow microfiber using a simple PDMS microfluidic chip. This study investigated the relationship between the wall thicknesses of alginate hollow fibers and enzyme activity. The thick wall of alginate hollow microfiber acted as a barrier which prevented enzyme leaching from the alginate matrix, without using any coating layers. Furthermore, it was also seen that the immobilized enzyme activity depended on the concentration of the metal ions in enzyme storage solutions.

1.2 Overview of Thesis Approach

The generation of a cylindrical microstructure like microfiber is simple and cost effective when using the PDMS-based microfluidic device. This method also works with different biomaterials and can be used to make different geometries such as solid microfiber or hollow microfiber. The different sizes of these microstructures are easy to control by adjusting the flow rate without re-tooling [1]. In addition, the PDMS microfluidic

chip can be fabricated in normal atmospheric conditions. Furthermore, neither pre-polymer nor nontoxic chemical reagents are needed. There is no exposure to high voltage, high temperature, or high pressure for the fabrication. Therefore, it is suitable for cells and various sensitive biocatalyst immobilizations. These biocatalyst-loaded microstructures can then be used as bioreactors for sensing or as scaffold for tissue engineering applications.

The PDMS microfluidic chip used for fabrication contained three inlets and one main outlet microchannels. Alginate solution was introduced in the branched channels and aqueous calcium chloride ($CaCl_2$) solution was introduced into the main inlet channel. When the two fluids contacted each other at the channels intersection, gelation occurred at the interface where Ca^{2+} ions diffused and bound to carboxylic groups of sodium alginate [2]. After sufficient residence time of polymerization, the alginate microfiber was spontaneously extruded from the microchannel without the assistance of high pressure. Unlike other studies that needed re-tooling to adjust the size of microfibers, in this work, the sizes of microfibers were controllable by simply adjusting core flow ($CaCl_2$) and sheath flow (sodium alginate). The relationships between flow rate and diameter characterization are presented in Chapter 3.

The alginate hollow fiber was then used as a bioreactor that entrapped the enzyme. Glucose oxidase (GOx) was chosen as the model enzyme for enzyme immobilization. GOx is a diametric glycoprotein that catalyzes the oxidation reaction of β-D-glucose to D-glucono-δ-lactone and H_2O_2 [3]. The molecular weight of GOx is approximately 130-175 kDa and it is active in a wide range of pH (5.0-7.0) [3]. GOx is a common enzyme in many academic research and industrial applications because it is low cost, easily accessible, reusable, and highly stable [3]. Moreover, its chemistry is well understood. The immobilized enzyme activity of GOx was examined using a colorimetric

assay. When the wall thickness of alginate hollow microfiber increased, the result showed that the biomaterial entrapped the enzyme more efficiently.

Chapter 2

Background and Literature Review

2.1 Enzyme Immobilization Methods

Enzyme immobilization is a method to restrict mobility of enzymes in a confined space of polymer matrices or to bind enzymes to carrier biomaterials. Enzyme immobilization has developed steadily and has become very important in fields like biotechnology, pharmaceutics, environmental industry, biomedical sciences, and food technologies [4-6]. The advantages of biocatalyst immobilization are as follows: 1) Significantly reduced cost, 2) Biocatalyst protected in hash conditions; 3) Prolonged enzyme viability; 4) Increased enzyme stability; and 5) Reusability [6]. In order to use enzymes in a wide range of different pH or temperature environments, their stability and half-life time must improve.

Many immobilized methods have been developed in previous studies. In this review, the most common methods are described in detail: physical adsorption, entrapment, and attachment via covalent linkage (Figure 2.1).

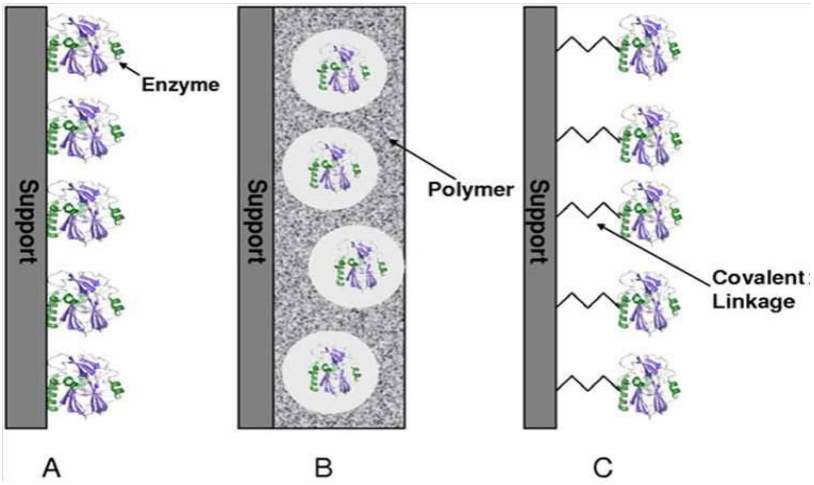

Figure 2.1 Three common enzyme immobilization methods: (A) physical absorption; (B) entrapment; (C) covalent binding [5].

2.1.1 Physical Adsorption

Enzymes are immobilized via physical adsorption based on weak binding forces (hydrogen bonds, salt linkages, and van der Waals forces) between enzymes and hydrophobic surface carriers. Physical adsorption is simple, cost effective, and causes no change of enzyme conformation that can affect enzyme activity. However, due to weak binding between the biocatalyst and the surface of the carrier, the immobilized enzymes can leak significantly from the carriers. This leak is triggered by any minor change in microenvironment such as temperature, pH, or ionic strength. In addition, it is very difficult to control biocatalyst molecules as they bind to substrate materials, and this unstable bonding process causes low reproducibility. Therefore, this method is only used in few applications [6].

2.1.2 Covalent Binding

In the covalent binding method, the enzyme forms a strong covalent bond with its support matrix by using chemical crosslinking reagents. In contrast to physical adsorption, the covalent bonds between enzymes and supportive matrices are more stable. This bond stability can prevent enzymes from leaking out of their support substrates. The usability of immobilized enzymes depends on the direction in which the enzyme binds to its substrates. It must bind correctly to perform at its highest enzymatic activity [6]. There are two approaches that allow enzymes to bind to the support matrix: 1) the enzyme directly binds to a functional group of support substrates without any surface modification; 2) the surface of the substrate is chemically modified prior to binding in order to allow the enzyme to bind to an active functional group of substrate [6]. The common support substrates usually include agarose, cellulose, poly(vinyl chloride), and porous glass. The most common binding side chains are lysine(ε-amino group), cysteine (thiol group), aspartic, and glutamic acids (carboxylic group) [6].

However, the use of chemical reagents may affect the active site of the immobilized enzyme. The change of the enzyme's conformational structure leads to reduced enzyme activity or even completed loss of enzymatic activity.

2.1.3 Entrapment Technique

Entrapment is a method in which the biocatalysts are caged but still the molecules are free within the confined core space of the hydrogel support matrix or inside the walls of a fiber. The most important advantage of this method is a minimum decrease in immobilized enzyme activity. Unlike covalent binding and physical adsorption, the immobilized enzyme itself does not bind to a support matrix or gel. In addition, enzyme immobilization does not require any chemical modifications. Therefore, the conformation of the enzyme and the active center of enzyme activity remain intact [6]. The other advantage of this technique is the ability to immobilize multiple biocatalyst components without having to consider the negative effects of the multiplied biocatalysts on each other [6].

The limitations of the entrapment method strictly depend on the support material. The low loading capacity of immobilized molecules is affected by diffusion limitation, damage on the support material, or the inherent pore size of the support material [6]. If the pore size of the supporting material is too small compared to the immobilized molecule, the biocatalyst cannot dissociate from the matrix to carry out its enzymatic activities. In contrast, if the supporting material has large pores, the immobilized enzyme can easily leach from the matrix, and this leads to low loading capacity. Therefore, choosing a suitable support material is the most essential factor in the entrapment method. The most common support materials that have been used include: alginate, chitosan, collagen, gelatin, carrageenan, polyurethane, etc. [6, 7].

A suitable support material must be biocompatible, nontoxic for immobilized biocatalysts and their products, and support high loading capacity. In addition, chemical and physical properties of supporting material such as porosity, biological stability, swelling behavior, biodegradability, and optimal mechanical strength are also important.

2.2 Alginate Biomaterial

The use of biomaterials has widely increased in tissue engineering and medical applications. These are developed to replace the loss of living tissue and to recover the natural function of these tissues that may be caused due to diseases or trauma. Two types of biomaterials are natural polymer and synthetic polymer. Natural or synthetic, a suitable biomaterial must be biocompatible, biodegradable, and low in toxicity [8, 9]. Therefore, natural biopolymers have been applied more widely compared to synthetic polymers because of their inherent biocompatibility and their ability to mimic biological environment in the host tissue.

Alginate is a natural polymer that derives from brown seaweed or from bacterial biosynthesis [9]. The alginate isolation process is shown in Figure 2.2.

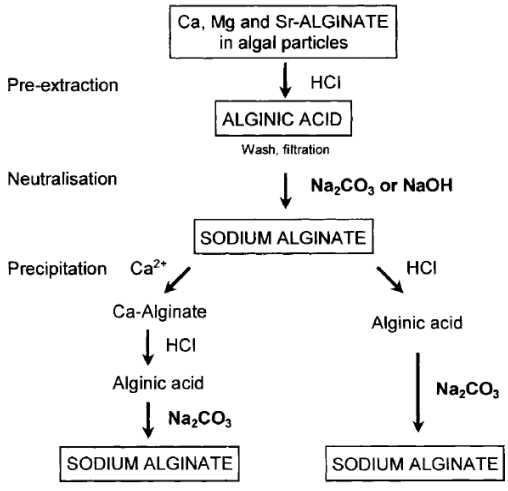

Figure 2.2 The general process of alginate isolation from seaweeds [10].

As indicated in Figure 2.3, the major components of alginate are copolymers α-L-guluronic acid (G) and (1-4)-β-D-mannuronic acid (M) [10]. The length of G block and M block contents are different in alginate extracted from different sources or from different parts of marine algae species [10].

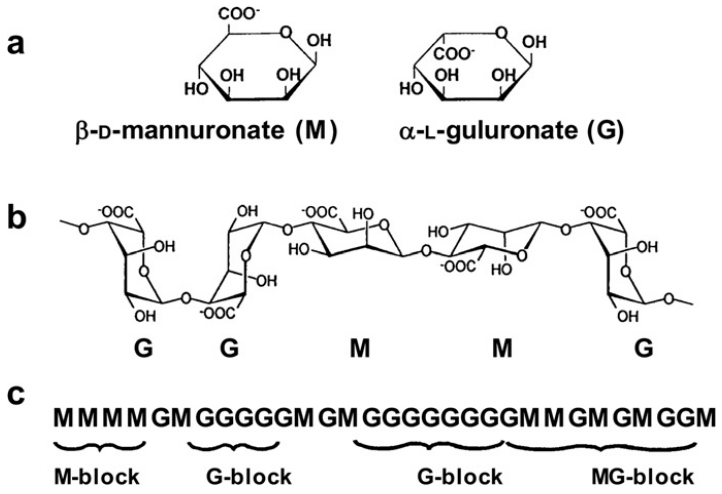

Figure 2.3 The chemical structure of alginate contains mannuronate (M) blocks and guluronate (G) blocks [11].

2.2.1 Biocompatibility of Alginate

It has been reported that alginate can act as an immune barrier to protect the transplanted cells from attack of the host immune system. The biocompatibility of alginate has been studied in both *in vivo* and *in vitro*; the studies have shown that the different ratios of intrinsic components of alginate biomaterials are responsible for inflammation response [12-16]. For example, a study [12] reported that different ratios of G block and M block, and alternating MG blocks of alginate stimulate necrosis factor-a, interleukin-6, and interleukin-1. Their conclusion stated that alginate with low G block content stimulated cytokine response 10 times higher than the one with high G block content. The

biocompatible property of alginate is also affected by the purity of alginate. Comparing to unpurified alginate, the purified alginate does not cause a mitogenic reaction in both *in vivo* and *in vitro* when alginate crosslinks with divalent cations [9]. The biocompatibility of alginate biomaterial also depends on its permeability behavior which can be controlled by adjusting M blocks. In an animal model with high macrophage reactivity, when the alginate contained approximately 68% of M-residues it showed the absence of mitogenic reaction. The stability and low permeability of the material protected the immobilized cells from attack of the immune system [16]. The alginate toxicity only happens due to contamination or impurity of the biomaterial [16, 17].

2.2.2 Biodegradability of Alginate

Alginate itself is an intrinsic non-degradable biomaterial without the presence of alginase enzyme that has the function to cleave the polymer chains of alginate polymer [9]. Biodegradation rate of alginate is very slow and uncontrollable [9, 18]. When alginate hydrogel is formed via ionic crosslink agents, the gel can be easily dissolved in the media. This is due to an exchange reaction that occurs between the monovalent cations present in the surrounding media and the divalent cations of gel matrix. This reaction leads to the release of divalent cations from the hydrogel matrix of alginate. Although alginate hydrogel can be dissolved, it cannot be completely removed from the host body because alginate biomaterials release strands that are higher in molecular weight than the maximum threshold of the kidney's clearance [9].

Biodegradable property of alginate gel in a physiological microenvironment can be improved by partially oxidizing polymer chains of alginate. The partial oxidized alginate can degrade in a controllable manner in aqueous media, and it has been widely used as a carrier for drug molecules to target a specific location *in vivo*. An alternative alginate hydrogel can be fabricated by oxidizing the polymer chain with sodium periodate

[18]. The cleavage of the carbon-carbon bond of the cis-diol group of urinate residue is achieved by sodium periodate and leads to alternation in the polymer chain conformation. Once the chain conformation of the polymer changes, it increases hydrolysis ability of the alginate polymer in aqueous solution. In addition, pH and temperature are also critical factors that control degradation rate of oxidized alginate. The application of alginate-derived hydrogel yields better results than pure alginate hydrogel when used to replace a cartilage-like tissue [18].

2.2.3 Methods of Alginate Hydrogel Formation

2.2.3.1 Ionic crosslinking method

The most simple and common method of alginate hydrogel formation is ionic crosslinking by using chemical agents that contain divalent cations. During the hydrogel formation, only the G block of alginate is involved in the crosslinking with cations [9]. The divalent cations bind solely to the G block of the alginate chain and form high degree coordination with these divalent cations. The ionic crosslink between chemical divalent cations and the G block of alginate is described as an “egg-box” model which is indicated in Figure 2.4.

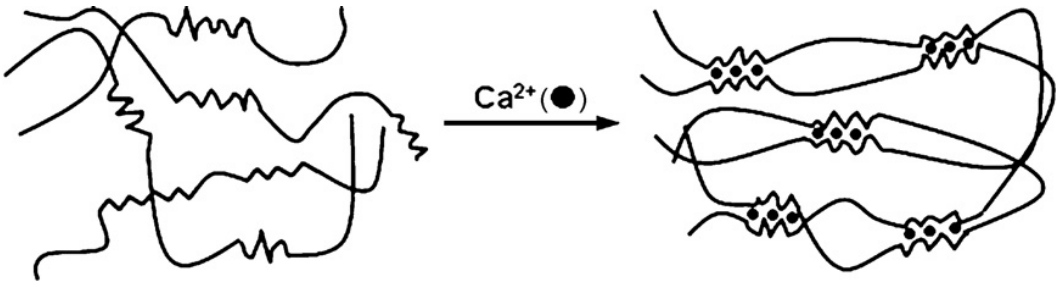

Figure 2.4 The “egg-box” model describes an ionic crosslink of divalent cations and the G chain of the alginate. Only the G block is involved in this ionic crosslink [9].

The strong affinity of alginate with different divalent cations is described by the following order: Pb, Cu, Cd, Ba, Br, Ca, Co, Ni, Zn, Mn [19]. Based on the affinity profile of divalent cations, when Ba^{2+} crosslinks with a high G block alginate gel, the hydrogel is more stable and has a better mechanical strength compared to Ca^{2+} ions. The size of Ba-bead alginate decreases and its permeability also reduces to immunoglobulin G protein [19]. However, Ba^{2+} ions can inhibit K^{+} channels of the biomembrane when its concentration is greater than 5-10 mM [19]. In addition, strontium ions (Sr^{2+}) are nontoxic in the physiological condition. It can be a suitable divalent cations when crosslinked with alginate [19].

Different divalent cations affect stability, mechanical strength, and permeability of the alginate hydrogel. The common chemical agents that have been used to crosslink with alginate biopolymer are calcium chloride ($CaCl_2$), calcium sulfate ($CaSO_4$), and calcium carbonate ($CaCO_3$) [9]. Different chemical agents have different effects on the gelation of alginate. For example, $CaCl_2$ is a highly soluble chemical reagent; Ca^{2+} of $CaCl_2$ crosslinks with alginate via “diffusion method” [10] and rapidly increases the rate of gelation [9, 10]. In contrast, the low solubility of the chemical agents, $CaSO_4$ and $CaCO_3$, can slow the gelation rate of alginate hydrogel formation. These chemical agents crosslink with alginate via the “internal setting method” [10]. The glucono-δ-lactone causes the divalent cations, Ca^{2+}, to dissociate and then the Ca^{2+} ions can coordinate with the G block of alginate to form alginate hydrogel [9]. At low temperatures, the ionic crosslink between divalent cations and the G chain of alginate becomes slower. The slow gelation process subsequently forms better network structure between the cations and G-chains. In addition, alginate material contains high G block which forms strong mechanical strength and high stiffness [9, 20].

In a physiological microenvironment, calcium alginate hydrogel usually swells in an osmotic condition. Its pore sizes increase and become more permeable which can lead to destabilization and rupture of the hydrogel. Under this condition, the divalent cations are gradually released from the gel and undergo an exchange reaction with monovalent ions in surrounding media. This reaction is a limitation that can be eliminated by coating with polycations layer. However, most common available polycations cause toxicity to the cells and fibrotic overgrowth [19].

2.2.3.2 Crosslink via covalent bond

Alginate can also form hydrogel by using covalent crosslinking reagents. In the ionic crosslinking method, the hydrogel behaves differently with the same amount of stress applied. In the covalent crosslinking method, when stress is applied the alginate gel is relaxed and water molecules migrate but cannot dissociate from the hydrogel matrix. Instead, the strong covalent bonds of these molecules can reform and the gel becomes an “elastic deformation” [9]. Several covalent crosslinking reagents used in this method can be toxic to immobilized biological molecules. In addition, unreacted components of these chemical agents must be washed out completely from the gel to avoid inducing immune response *in vivo* [9].

The properties of chemical crosslinking reagents play an important role to control the behavior of alginate hydrogel. When the molecular weight of the crosslinking agent changes, it leads to a change in the crosslinking density and its chain length. These factors affect the mechanical and swelling properties of alginate hydrogel [21]. Alginate gel properties can also be controlled in a more efficient way by using multifunctional crosslinking reagents. For example, in Lee et al. [22] study, they investigated whether mechanical stiffness and degradation were different when they changed the covalent crosslinking reagents which were the multifunctional molecule, PAG (poly (aldehyde

guluronate))/ PAH (poly(acrylamide-co-hydrazide)), and the bifunctional molecule, PAG/AAD (adipic acid dihydrazide). PAH contained more multiple attachment points than AAD even though both contained the same concentration of the functional groups. The gel contained higher mechanical properties with a slow degradation rate under effect of multifunctional PAG/PAH gel compared to bifunctional PAG/AAD gel.

2.2.3.3 Thermal sensitive hydrogel

Thermal sensitive hydrogel has been developed and widely used in drug delivery applications. Thermal gelation in drug delivery is dependent on the swelling properties of the hydrogel at different temperatures or different biological microenvironments. The thermal sensitive polymers act as carriers to deliver the drug in the host body, to sense localized temperature at a specific location, and swell to release the drug. Although alginate hydrogel is not an inherent temperature sensitive polymer, it still plays an important role in controlling the swelling when it is combined with another thermal sensitive polymer.

In Zhao et al. [23] study, they fabricated a sensitive thermal polymer named “thermo-sensitive semi-IPN hydrogel” which was formed by combining N-isopropylacrylamide (NIPAAm) and copolymer poly(ethylene glycol)-*co*-poly(ε-caprolactone) (PEG-*co*-PCL) via in situ copolymerization. The sodium alginate was added to the thermal hydrogel by using the UV irradiation technique. The study showed that sodium alginate was a main component of copolymer that affected the swelling property of the hydrogel. At a constant temperature, when the sodium alginate content increased the swelling ratio also increased. When sodium alginate content and temperature increased, the swelling ratio decreased. In addition, salt sensitivity of semi-IPN hydrogel also depended on the sodium alginate presence in the hydrogel. This study

also demonstrated that the mechanical property of thermo-sensitive hydrogel can be improved by presence of sodium alginate material.

2.2.4 Alginate Biomaterial Applications

2.2.4.1 Drug delivery

There are many drug molecules that contain small molecular weights. In an *in vivo* study, the challenge is to protect these micro/nano scale drug molecules to reach target locations/organs and release drug molecules. Alginate hydrogel inherently is a nanoporous matrix with approximately 5 nm pores [9]. Therefore, it allows many different small biological, chemical molecules, or drug molecules to diffuse easily through the alginate gel. The kinetic mechanism of drug release depends on primary and secondary bonding between drug molecules and alginate [9]. For example, an oxidized derived-alginate crosslinked with Ca^{2+} entrapped 89% flurbiprofen and it took 1.5 hours to release the drug molecules in phosphate buffer solution (pH 7.2) *in vitro*. However, when the oxidized alginate was ionic crosslinked with Ca^{2+} and then covalently crosslinked with adipic acid dihydrazide (ADH), it formed a novel alginate hydrogel that prolonged the time of drug release up to 8 hours. This controlled time of release depended on the appropriate concentration of ADH in alkaline dissolution media. This result can be explained by the increase of crosslinking density and reduction of hydrogel swelling. The increasing concentration of surrounding media such as HCl solution (pH 1.2) or phosphate buffer solution (pH 7.2) directly leads to reduction of swelling tendency and the rate of the release of the drug molecules [9, 24].

In addition, oxidized-derived alginate can control sequential delivery when multi-drugs are immobilized in the alginate beads [25]. For example, three drugs, methotrexate, doxorubicin, and mitoxantrone, were encapsulated in the oxidized alginate beads. Methotrexate easily diffused through alginate hydrogel because its chemical

structure did not interact with alginate. On the other hand, doxorubicin crosslinked to alginate gel via covalent bonds. Therefore, the drug only released from the gel when it cleaved the crosslinker of alginate via chemical hydrolysis. In contrast, mitoxantrone had to dissociate and cleave the ionic bond with alginate to allow the release to localized targets [9, 25].

In drug delivery applications, alginate can combine with other biological natural polymers such as chitosan to form ionic complexes and can be used as sufficient drug carriers. Chitosan is a cationic polymer that is derived from chitin and contains a repeated structure of (1,4)-β-D-glucosamine. Many available commercial chitosans contain 80% β-D-glucosamine and 20% N-acetyl-β-D-glucosamine [9]. Similar to alginate polymer, biocompatibility and other biological properties of chitosan are suitable in various biomedical and pharmaceutical applications. In previous study [26], multi-particulate alginate/chitosan system acted as a colonic drug delivery system. At different biological conditions, this multi-particulate system released the drug at different rates. For example, in enteric environment at pH 7.5, the degree of swelling of the alginate/chitosan system was higher and subsequently the rate of the drug release was faster compared to an environment that would mimic gastric conditions (pH 1.2).

2.2.4.2 Biocatalyst delivery

Alginate can be considered as the most suitable sensitive protein carrier in the biological system because alginate-based material can protect and minimize protein denaturation in undesirable conditions. Alginate gel itself is a porous matrix and hydrophilic polymer; proteins can be easily released from the gel with a rapid rate. Protein release rate also depends on the degradation rate of alginate gel. The proteins with a high isoelectric point (pI) such as lysozyme and chymotrypsin can efficiently encapsulate the alginate microsphere via a physical crosslink with sodium alginate. This

crosslink method leads to more sustained release and rapid loading of proteins in alginate microspheres [9].

The immobilization efficiency and release rate of biocatalysts from hydrogel mainly depend on interactions between the biocatalyst and its carrier. For instance, in a study, insulin molecules were delivered to the localized host intestine by co-encapsulating with anionic polymer such as cellulose acetate phthalate, polyphosphate, or dextran sulfate in alginate hydrogel and then coated with cationic chitosan. These insulin molecules were protected by these coating layers in a low pH location in the body such as stomach. It also showed that these insulin molecules were successfully released locally in the intestine [9, 27]. The other delivery system was developed from PLGA/alginate combination microsphere/hydrogel [28]. In this study, the PLGA microsphere contained model protein bovine serum albumin (BSA). These protein-loaded microspheres were then encapsulated in alginate hydrogel. *In vivo*, the result showed that this combined microsphere/hydrogel system protected the target molecules from attack of phagocytes (Figure 2.5).

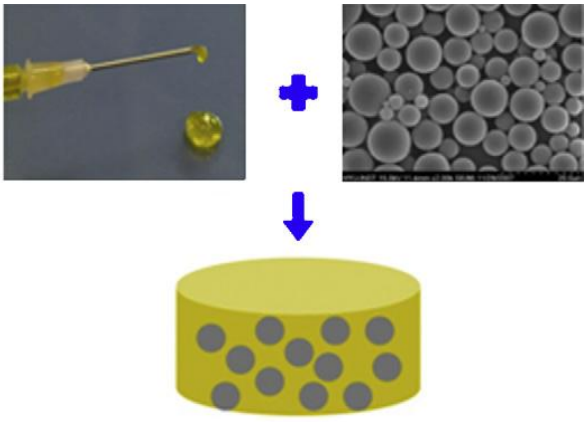

Figure 2.5 PLGA microsphere/alginate hydrogel combined system was used as the carrier for biocatalyst delivery [9].

2.3 Fiber Microstructure Fabrication Techniques

In tissue engineering and immobilization applications, there are many different techniques that can be used to fabricate microfibers from natural polymers or synthetic polymers such as electrospinning, wetspinning, interfacial complexation, meltspinning, and microfluidic-based device (Figure 2.6). Each method contains advantages and limitations.

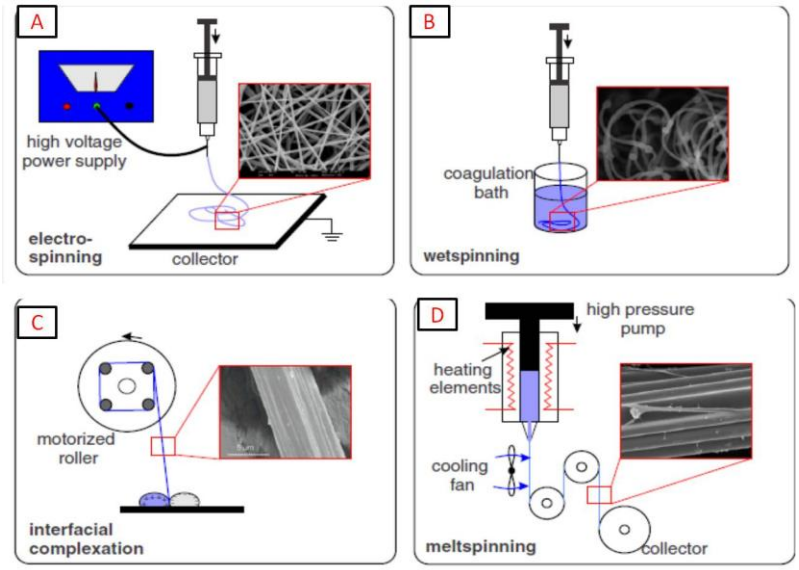

Figure 2.6 Microfiber can be fabricated by various techniques: (A) electrospinning, (B) wetspinning, (C) interfacial complexation, and (D) meltspinning [29].

2.3.1 Electrospinning Technique

Theoretically, electrospinning is a method in which the polymeric solution is drawn from the needle and stretched in uniaxial direction by electrostatic force with a high voltage [30]. The collected fibers contain various diameters from nano to micrometers. The sizes of fiber in electrospinning can be controlled by physical properties of polymer,

applied electric fields, flow rate, and the distance between the tip of the needle and collector [29].

The advantages of this technique are: 1) simplicity, 2) ease in controlling size of fibers, 3) and no need for a chemical agent or high temperature [29]. However, for enzyme immobilization, this technique is not suitable because the fibers fabricate with very high density and it is difficult to control the density of these fibers [29]. In addition, the high electric field such as 1-2 kV/cm can be dangerous for the cells or sensitive biological molecules [29].

2.3.2 Wetspinning Technique

In contrast to electrospinning technique, the wetspinning method can fabricate a long fiber with a wide range of diameters from 30 to 600 μm [29]. The concept of this method is based on polymerization of pre-polymer solution in coagulation bath which contains chemical solvent or nonsolvent. The pre-polymer solution can be injected manually, with a syringe pump, or by applying pressure. The various natural and synthetic polymers have been studied using this techniques such as alginate, collagen, chitosan, polycaprolactone (PCL) [29].

The diameter of fiber can be controlled by the size of needle, flow rate, or composition of polymer. Although this method is simple, the immobilized biological molecules may be harmed because they must stay in the chemical solution for long period of time [29].

2.3.3. Interfacial Polyelectrolyte Complexation Technique

The interfacial complexation technique fabricates microfibers based on the opposite charges of polyelectrolyte solutions such as chitosan, sodium alginate, and hyaluronic acid. The fiber diameters are in the range of 10-20 μm. The size of fiber can

be controlled by adjusting the polyelectrolyte concentration and the interfacial area [29]. However, this method is complex and it only works well with a few types of polymers [29].

2.3.4 Meltspinning Technique

Meltspinning is a method where the polymer is heated at an extremely high temperature, and the generated microfiber is then extruded from the spinneret after a resident time. This technique is suitable for synthetic polymers that have a high melting point. Meltspinning requires a high temperature range and a high pressure to extrude the polymeric microfiber through the spinneret. Therefore, the meltspinning method cannot be used for enzyme immobilization.

2.3.5 Microfluidic Fiber Synthesis

The microfiber formation in a microfluidic channel is based on a coaxial flow reaction between a pre-polymer and a crosslink agent. These two fluids are introduced at the inlets; they then pass through the microfluidic channels and merge at the intersection. At the gelation phase, the divalent cations of the chemical agent exchange and crosslink with the pre-polymer chain via the diffusion or internal gelation. After sufficient residence time, the microfiber can spontaneously extrude out from the outlet microchannel (Figure 2.7).

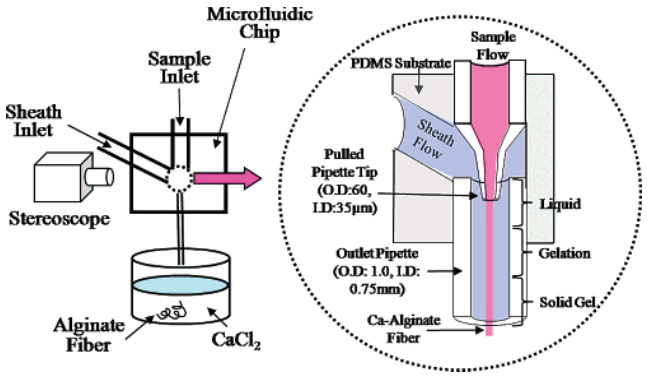

Figure 2.7 The scheme illustrates microfiber synthesis and the gelation process [2].

By using this method, the microfiber generation can be applied for both natural and synthetic polymers. In addition, the fiber diameter is easy to control by changing the flow rate, size of microfluidic channels, and viscosity of pre-polymers [29, 31]. The structures of microfluidic devices are easy to modify depending on specific applications. For example, for enzyme immobilization, the hollow fiber has been fabricated by a device that contained two inlets and one main outlet [32]. In another study, for drug and cell co-encapsulation, the hydrogel fiber was generated by a device that consisted of three inlets and three dispersing chambers [33]. In Yamada et al. [34] study, they designed a complex microfluidic device that had seven inlets and one main outlet. This device was then used to fabricate the continuously anisotropic calcium alginate fiber. These anisotropic alginate fibers were distributed to control the direction of cell proliferation.

The microfluidic device as a fiber-based technique is more suitable for enzyme immobilization compared to other previously mentioned fiber-based techniques. Its advantages include: 1) simplicity; 2) controllable flow rate; 3) no need of high temperature; 4) no need for high electric field; and 5) no need to expose the immobilized molecules to chemical agents for a long period of time.

Despite its weak mechanical properties, continuous fiber synthesis by the microfluidic device is a promising advancement. It provides a great benefit for different biological applications like in regenerative medicine and tissue engineering.

2.3.5.1 Microfluidic device fabrication

Polydimethylsiloxane (PDMS) is a silicone elastomeric material that has been used to fabricate microfluidic devices. The advantages of PDMS are: 1) low cost, 2) thermal stability, 3) gas permeability, 4) easy manipulation, and 5) chemical inertness [35]. Traditionally, microfluidic devices have been fabricated by common methods such

as soft lithography or photolithography. Recently, a simple microfluidic device was fabricated by using a glass capillary-based system [1, 36].

2.3.5.1.1 PDMS microfluidic device fabrication using soft lithography

In the soft lithography approach, the microchannels are fabricated by molding and prototyping. In many studies, the soft lithography method is used to fabricate complex devices [37, 38]. For example, a study designed a complex device that could fabricate various microfibers of different compositions at the same time [37]. It was a single platform microfluidic device that consisted of 5 coaxial-flow channels and 12 mixers rectangular channels (Figure 2.8 (top)). The rectangular channel mixers were fabricated easily by soft lithography.

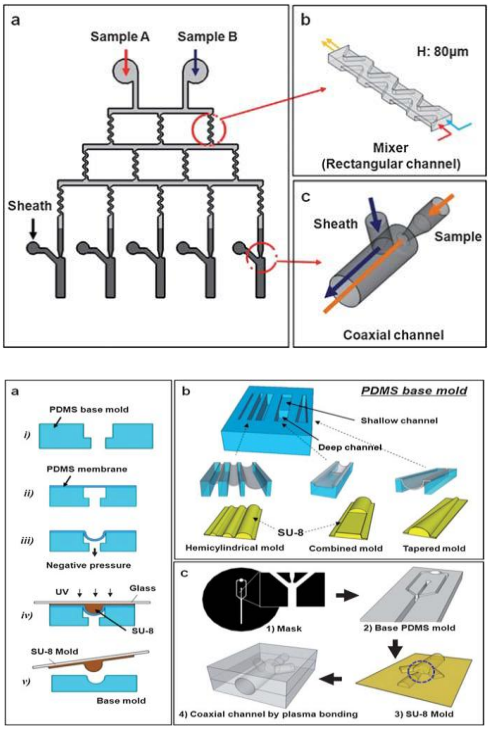

Figure 2.8 (Top) The complex device consists of 12 mixer rectangular channels and 5 coaxial channels. (Bottom) The scheme describes the additional steps to modify the PDMS rectangular channel into a cylindrical channel [37].

However, a cylindrical channel could not be directly fabricated using this technique. Instead, several additional steps were required to achieve a cylindrical shape (Figure 2.8 (bottom)). Therefore, the disadvantages of the soft lithography method are that it is: 1) complicated, 2) time consuming with multisteps, 3) expensive, and 4) requires cleanroom environment.

2.3.5.3 PDMS microfluidic device fabrication using glass capillary tube

In 2005, Jeong et al. [36] reported a simple method to fabricate cylindrical microchannels by glass capillaries. This simple microfluidic device contained two inlet channels and one glass capillary tube as the main outlet (Figure 2.9).

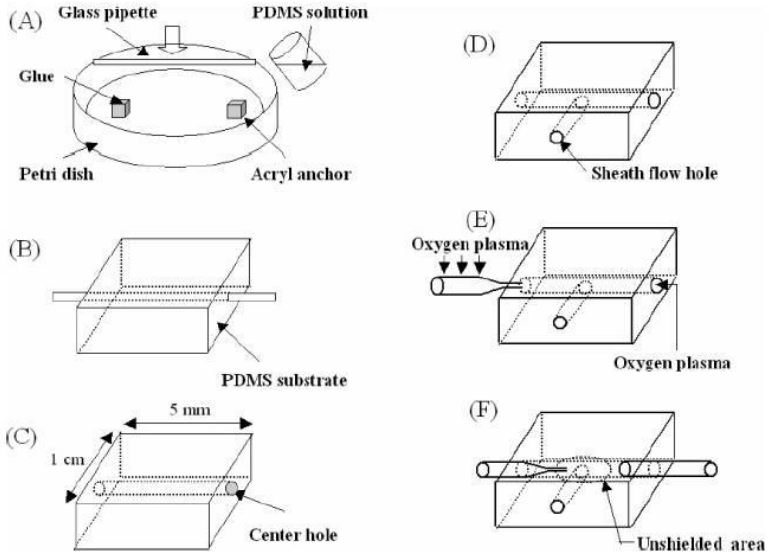

Figure 2.9 The scheme describes a simple microfluidic-based platform with glass capillary [38]. Microfiber synthesis by this method is based on wetting fluid property [37].

The advantages of this method are simplicity and rapid fabrication. The microfluidic device could be fabricated in a wet lab environment, and the fiber size could

be controlled by changing the flow rate. This microfluidic-based platform has been used in various studies such as enzyme-loaded microfiber [32, 36], PLGA microfiber for 3D cell culture [39], alginate microfiber acting as a cell carrier [2], and to control the cell proliferate orientation [31].

The generated microfibers using the glass capillary-based microfluidic device depend on the wetting fluid property [38]. Core-shell jets form and flow down the walls of the capillary if a device uses multiphase streams for the sheath flow. These can be formed into hollow microfibers when introduced to UV radiation [38].

2.4 Conclusions

This chapter introduces state of the art techniques in enzyme immobilization. Entrapment is the currently preferred method for immobilizing enzymes because it does not affect enzyme conformation. Alginate is well suited for enzyme entrapment; its chemical and physical properties support high loading capacity. This chapter also provides a clear and concise background on microfluidics and microfiber fabrication. Alginate microfibers can be fabricated in many ways. Of all current practices, the microfiber-based microfluidic technique is the most promising development in enzyme immobilizing fiber production. This technique does not require a high electric field, high temperatures, or any chemical exposure in order to generate these fibers. Alginate microfibers are, therefore, easy to produce.

Chapter 3

Microfluidic Channel Approach

Using the glass microcapillary-based system, the coaxial flow mechanism results into synthesis of microparticles and microfibers without clogging. A major drawback of this method is its labor-intensive nature, requirement for certain skillset, and need for specialized tools [37]. The aim of our work was to design a non-lithographic PDMS microfluidic device based on a simple technique using a template. This template method is simple, rapid, and cost effective. Similar to the glass capillary-based system, our device can synthesize microfibers by the coaxial flow mechanism. The generated microfiber can extrude out from the outlet after polymerization without clogging in the channel. Unlike the glass capillary-based microfluidic device, all inlet and outlet microchannels are in PDMS mold. Several device fabrication approaches are presented in this chapter including different template designs, limitations, and methods to overcome backflow.

The critical step in our template method was to ensure that all templates could be easily extracted without contorting or blocking the microchannels. Our microfluidic device contained three inlets and one main outlet. The device template was made from the small, cost effective capillaries and aluminum wires. A 10% PDMS solution was then poured completely over the template and was cured at 150 ˚C. All the templates were then extracted, and oxygen plasma was performed to add silanol (SiOH) groups to the surface, making these hydrophilic. This allowed the water to wet the PDMS surface.

3.1 Template Platform Methods and Challenges

3.1.1. Approach 1: Y-shaped Device

The design of this microfluidic device had three inlets and one outlet channel coming together in Y-shape. The template was prepared by tightly twisting three separate 300 µm aluminum wires together (Figure 3.1).

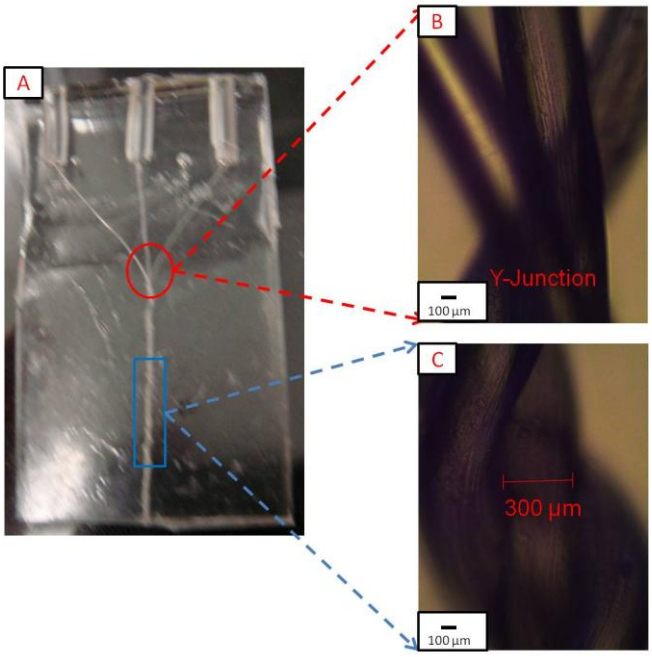

Figure 3.1 (A) The Y-shaped device had three inlets and one main outlet. The optical micrographs show (B) the intersection of the inlet microchannels and (C) the outlet channel.

Challenges:

There was no opening at the intersection due to PDMS blockage at the junction. The water could not pass through the Y-intersection. At the low laminar flow rate, the backflow occurred at the inlets. In some cases, the outlet surface of the microchannel got

rupture after extracting the templates. Therefore, this device was not an optimal device for microfiber fabrication.

3.1.2. Approach 2: T-shaped Device

The aim of this approach was to control the opening at the intersection (T-junction).The template was prepared similar to the T-shape shown in Figure 3.2. The diameters of the inlet microchannels were approximately 300 µm, and the diameter of the outlet microchannel was 400 µm. The T-template was secured on the Petri dish using tape.

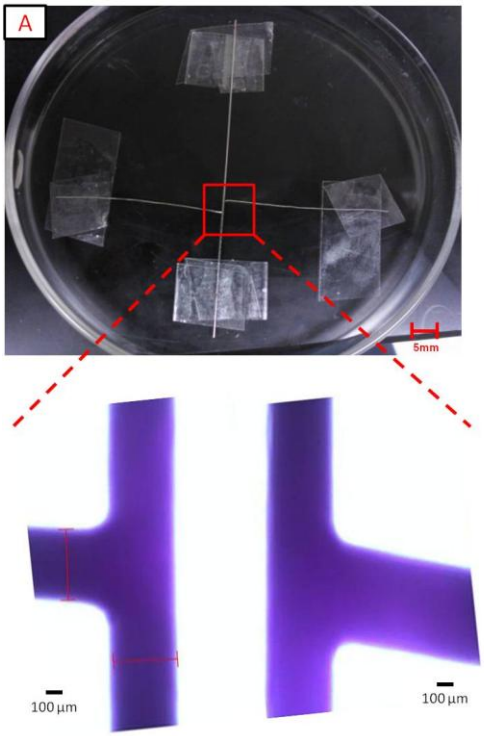

Figure 3.2 The optical micrograph shows PDMS microfluidic device with three inlets and one outlet. The microchannels connect to each other at the T-junction.

Challenges:

The connections between the inlet and outlet channels were observed with an optical light microscope. In Figure 3.2, it shows a secure connection without PDMS blocking the T-junction. It was an improvement from the previous Y-shaped device. However, it was not easy to adjust the opening at T-junction of the template because the size of the wires was so small. All of the pieces of the template could be easily extracted after curing at 150 ˚C, and no rupture occurred on the surface of the channels.

After performing hydrophilization with oxygen plasma, the flows of fluid in the fabricated channels were tested with water. The device was vertically situated in order to allow water to pass through easily. The limitation of this device was the backflow. As illustrated in Figure 3.3, water was injected in the inlet (3); red and blue dye solutions were introduced into inlet (1) and inlet (5). At the T-junction, red and blue dyed aqueous solutions flowed out of the device through inlet (3). There was no flow at the outlet channel (4).

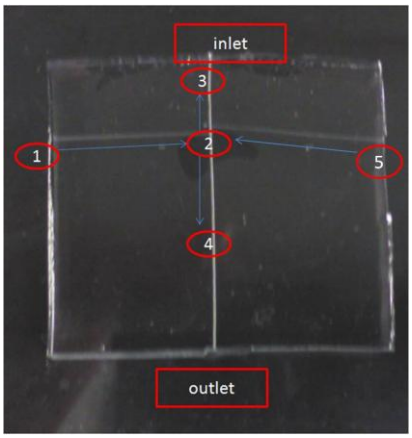

Figure 3.3 The fluids passed through the PDMS microchannels at a low laminar flow rate. The flow of the fluids was easily observed from the red and blue dyed solution. The dyes showed that water could pass through inlets (1) and (5); these fluids intersected at the T-junction (2). However, backflow occurred and pushed the fluids back to inlets.

3.1.3. Combating Backflow

A major drawback of the microfluidic devices was backflow. Backflow occurred in both the Y-shaped and T-shaped devices. In general, for microfiber fabrication purposes, backflow can cause polymerization inside microchannels and clogging during the gelation process.

The three main potential causes of backflow are: 1) the hydrophobic properties of PDMS, 2) the viscosity of the fluid, and 3) the diameter of microchannels. Firstly, although PDMS itself is hydrophobic, the surface was made hydrophilic through exposure to oxygen plasma. Therefore, the backflow cannot be attributed to the hydrophobicity of the PDMS polymer-based microchannels. Secondly, it is important to consider whether the viscosity of fluids can cause backflow. Water is considered an ideal fluid in most fluid dynamic studies. Therefore, in this experiment, we only used water to run the tests. At room temperature, the viscosity of water is 1 mPas [40], which is much lower compared to the 20-2000 cps (or 20-2000 mPas) viscosity of alginate solution [41]. Moreover, the PDMS device was vertically situated in order to reduce the contact surface area between the microchannels and the fluids. This reduced contact surface area allowed water to pass easily through the channels. Therefore, viscosity is not the main contributing factor of backflow.

To our knowledge, no previous studies have reported the relationship between backflow and diameter of PDMS channels. However, as we observed from both devices, the ratio of inlet to outlet diameter could be a main cause of backflow.

As we know, the fluid motion from upstream (inlet) to downstream (outlet) in the pipes or channels are described in the form of the continuity equation [42]:

$$v_i \, A_i \, = \, v_f A_f$$

A= cross section area

v = velocity

In our specific design, the cross section areas of three inlets (upstream) are equal. Therefore, we have:

$$v_1A_1 + v_2A_2 + v_3A_3 = v_fA_f$$

Because the diameters of these three inlets are equal (300 μm), we have:

$$3 * (v_i\ A_i) = \ v_fA_f$$

Assume the velocity of the flow at the inlet is as same that at the outlet channels. The assumption means that the velocity parameters can be neglected in the equation:

$$3 * (A_i) = \ A_f$$

It was thus concluded that backflow can be prevented by increasing the outlet diameter. However, if we increased the outlet microchannel to be three times as large as the diameter of the inlet channels, the new outlet microchannel would be unacceptably large. Therefore, our next approach was to design a device that would meet the following criteria: 1) allows fluid to merge at the intersection; 2) prevents backflow at inlets; 3) increases the diameter of the outer microchannel without it becoming too large.

3.2 Experimental Approach

3.2.1 The Displaced Y-shaped Device

To prevent backflow, the outlet channel diameter was approximately equal to the sum of the two branched inlet diameters. Unlike the Y-shaped device, the inlets of the displaced Y-shaped device were connected 1 mm away from the end of the outlet microchannel. The optimum microfluidic device fabrication is illustrated in Figure 3.4.

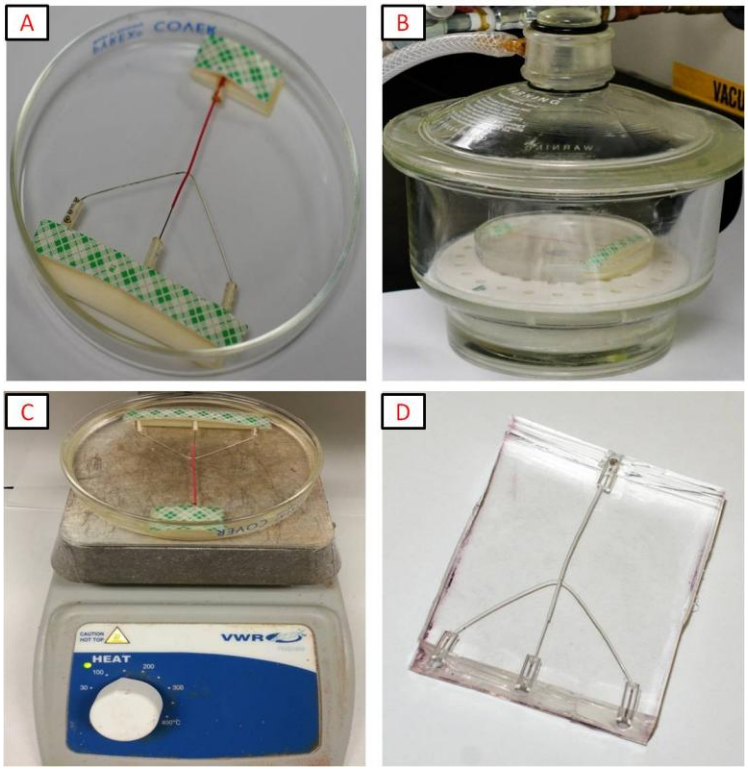

Figure 3.4 The steps to fabricate PDMS microfluidic device using the templates. (A) The template platform was formed as shown. (B) The template was fully covered by PDMS and then placed in a vacuum chamber. (C) The PDMS was cured at 150 ˚C. (D) All pieces of the template were extracted.

The process was, in essence, the use of the plastic hollow capillary tube as the outlet template. The diameter of the hollow capillary tube was 0.7 mm. A small hole was punched through the plastic capillary using a small BD needle (26 G x 5/8 inches). The distance from one end of plastic capillary to the hole was 1 mm. A straight aluminum wire was inserted through the hole. The diameter of the small wire was 0.40 mm. Then, the wire was bent at approximately a 45˚ angle to form a V-shape. For the middle inlet template, another piece of the small wire (0.40 mm diameter) was attached at the end of

the hollow plastic capillary. Finally, the bigger plastic capillaries (1 mm diameter) were inserted at the open-end of the three inlets and main outlet. The displaced Y-shaped template was secured on a glass Petri dish with double-side tape above and below the template.

Next, the template was completely covered by 10% PDMS pre-polymer. The Petri dish was then placed back into the vacuum chamber to eliminate all of the air bubbles. After that, the PDMS-based Petri dish was cured at 150 ˚C on the hot plate. Finally, after extracting the template, the PDMS device was exposed to oxygen plasma for 10-15 minutes in order to make the PDMS surface hydrophilic.

The final PDMS device contained three inlets and one main outlet. The lengths of the inlet and outlet microchannels were 3.3 cm and 4 cm. The displaced Y-shaped device was the optimum device for fabrication because the fluid could pass through the microchannels without backflow or PDMS blockage. In addition, the fabricated process was simple and rapid in the wet lab environment.

3.2.2 Fabrication of Alginate Hollow Microfiber

The alginate hollow microfiber was generated with alginate pre-polymer and a $CaCl_2$ solution. A 2% (w/v) sodium alginate solution was injected into the branched (left and right) channels. A 20 mM $CaCl_2$ aqueous solution was introduced into the core inlet channel as shown in Figure 3.5. The microfiber was formed inside the microfluidic channel via an ionic crosslink. The sodium alginate and $CaCl_2$ solution flowed down the PDMS microchannels and merged at the intersection. When the sodium alginate and $CaCl_2$ solution interfaced, the gelation process began instantaneously. Ca^{2+} divalent cations rapidly released from $CaCl_2$ solution, diffused into the alginate polymer, and attached to carboxylic groups of sodium alginate in an “egg-box” model.

The diameters of the alginate hollow fiber were controlled by core flow ($CaCl_2$) and sheath flow (2% alginate solution). To indicate the relationship between the flow rates and the diameters of alginate hollow fiber, two sets of experiments were performed: 1) varying core flow at the constant sheath flow and 2) varying sheath flow at the fixed core flow.

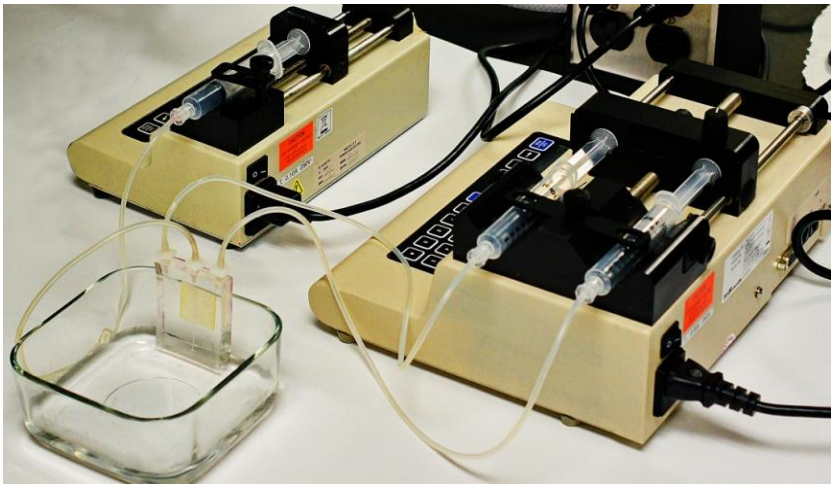

Figure 3.5 The experiment setup. A 2% alginate solution and 20 mM $CaCl_2$ are introduced into the branched inlets and main inlet channels. The alginate pre-polymer and $CaCl_2$ solution merge at intersection and polymerize via ionic crosslinking mechanism. The hollow microfiber is collated in 100 mM $CaCl_2$ in square beaker.

In the first experiment, the sheath flow was kept constant at 0.05 ml/min while the core flow rate varied as: 0.42, 0.50, 0.66, 0.75, and 0.90 ml/min. In the second experiment, the core flow was kept constant at 0.50 ml/min and the sheath flow was varied as: 0.01, 0.03, 0.05, 0.1, and 0.3 ml/min. The calcium alginate fibers were collected in the beaker containing 100 mM $CaCl_2$ solution. These fabricated alginate microfibers were then stored in 100 mM $CaCl_2$ for 24 hours.

After 24 hours, the physical property of calcium alginate fiber was investigated by the Scanning Electron Microscope (SEM). The hollow and symmetric geometries of the microfibers were observed by staining the fiber with a red dye. The diameters of the alginate microfibers were measured by an optical microscope. Along a single alginate hollow fiber approximately 4-6 cm in length, the inner and outer diameters were measured randomly at 10 different points. The wall thickness was determined by subtracting the inner diameter from the outer diameter. Each experiment was repeated in triplicates (n = 3). Finally, the parameters were expressed as means with standard deviation. The linear relationship of the flow rates and the diameters were reported.

3.3 Results

3.3.1 The Alginate Hollow Microfiber Characterization

The fiber can be fabricated continuously as long as the solutions enter at the inlets. The length of fibers was controllable as indicated in Figure 3.6.

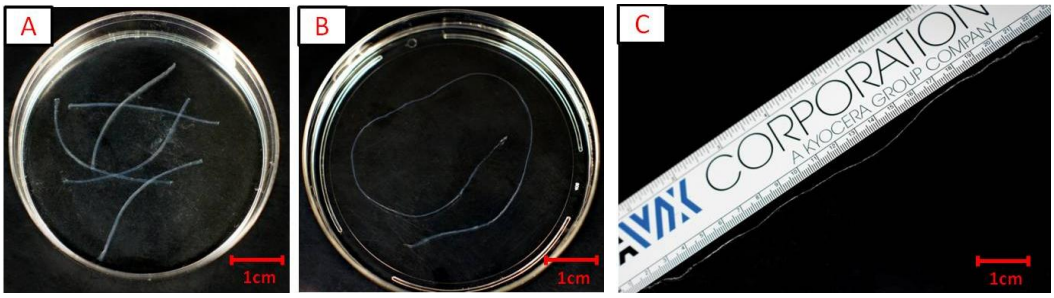

Figure 3.6 The alginate hollow fibers were kept in 100 mM $CaCl_2$ solution. The lengths of the fibers were controllable: (A) 4-6 cm. (B) and (C) The length of fiber can be up to 22 cm long.

The length of the fabricated fiber can be up to 22 cm as shown in Figure 3.6 (B) and (C). The optimal and repeatable length of the hollow fiber was 4-6 cm (Figure 3.6 (A)).

In the Figure 3.7, the shape of the alginate fiber was maintained consistently. The outer surface of the fiber was smooth; it did not show any sign of rupture, distortion, or abrasion. In dried form, the alginate microfiber shrank due to water loss.

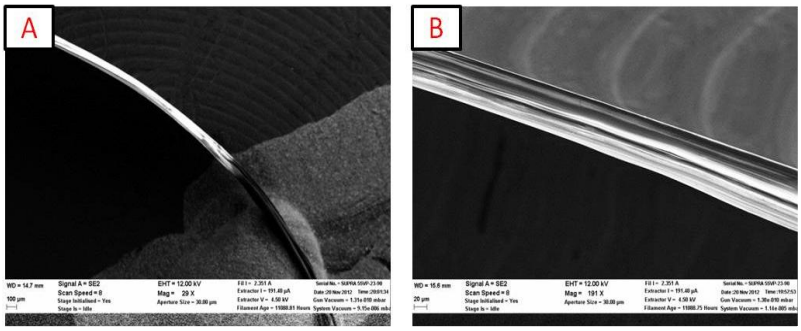

Figure 3.7 The outer surface of the alginate hollow microfiber was smooth without any distortion (SEM micrographs).

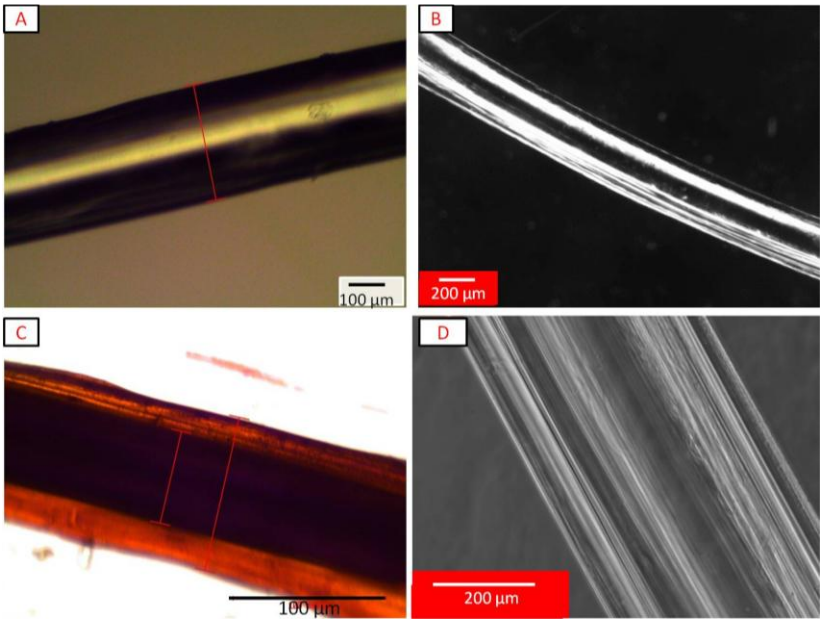

Figure 3.8 These micrographs demonstrate that the fabricated alginate fiber was hollow by using: (A) a light microscopy and (B) an optical microscopy. (C) The core space was stained with a red dye solution (the dried fiber). (D) The core space of the alginate fiber was smooth, and there was no clogging inside the microfiber.

The hollow and symmetric characteristics of the alginate fiber were investigated with light microscopy (Figure 3.8 (A)) and an optical microscopy (Figure 3.8 (B)). In these micrographs, the inner diameter and the wall thickness are clearly distinguishable from each other. In Figure 3.8 (C), the core space of a dried alginate fiber is stained and shows the red dark color to be different from the side wall. In addition, the optical micrograph shows that the core space of the hollow fiber is smooth and indicated no signs of rupture (Figure 3.8 (D)).

3.3.2 At the Constant Sheath Flow, the Core Flow Rate Affected the Internal Diameter and the Wall Thickness of the Hollow Fiber

In the first experiment, the sheath flow rate was constant at 0.05 ml/min, while the core flow rates of $CaCl_2$ were changed as: 0.42, 0.50, 0.66, 0.75, and 0.90 ml/min. At 0.42 ml/min, the internal diameter of the hollow fiber was smallest. In contrast, the internal diameter of the hollow fiber was largest at 0.90 ml/min. The changing of the internal diameter with increasing core flow rate is shown in Figure 3.9.

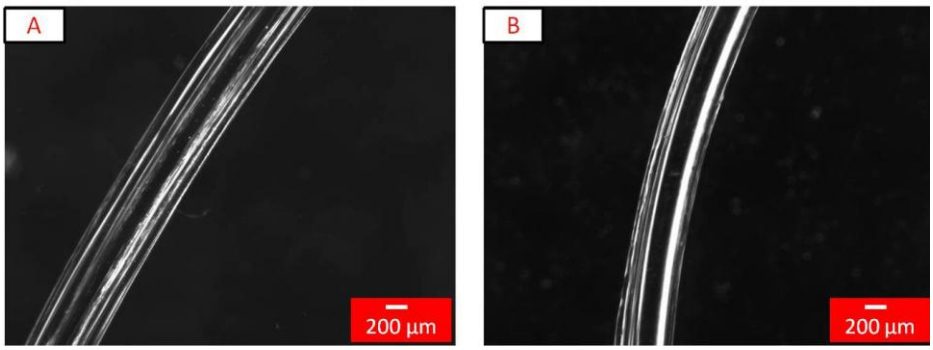

Figure 3.9 (A) At 0.42 ml/min, the internal diameter is approximately 134 ± 2.75 µm. (B) At 0.90 ml/min, the internal diameter is approximately 278 ± 78.83 µm.

The varying core flow rates affected the outer diameter, internal diameter, and wall thickness of the hollow fiber all differently. These relationships are indicated clearly

in Figure 3.10. The trend shows that the internal diameter of the hollow fiber increased proportionally when the core flow rate increased. The outer diameters were essentially unaffected by varying the core flow rates. The wall thickness of the alginate hollow fiber decreased with the increasing core flow rate.

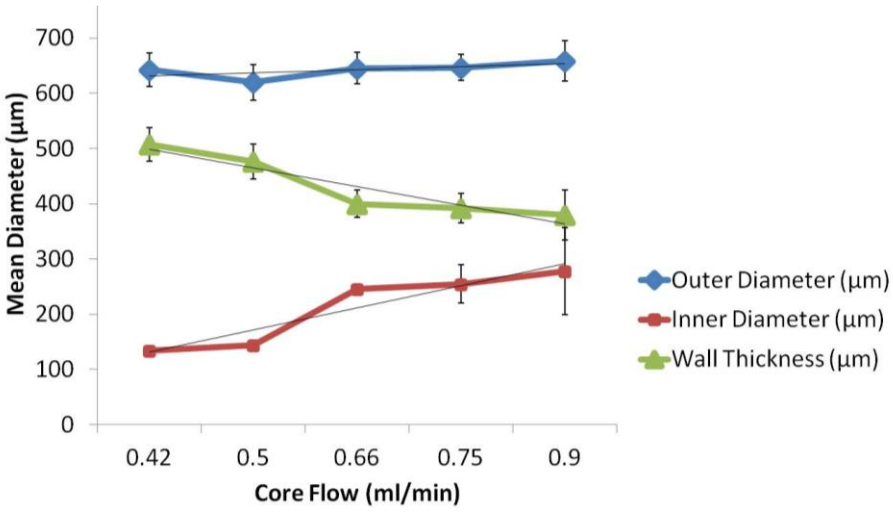

Figure 3.10 The relationships between the dimensions of the hollow microfibers and the core flow rates at the constant sheath flow of 0.05 ml/min. Bar: SD (n = 3)

3.3.3 At the Constant Core Flow, the Sheath Flow Rate Changed the Internal Diameter and the Wall Thickness of the Microfiber

At the constant core flow rate of 0.50 ml/min, the sheath flow rate was varied as: 0.01, 0.03, 0.05, 0.1, and 0.3 ml/min. At 0.01 ml/min, the largest diameter was 252 ± 26.2 µm (Figure 3.11 (A)). At 0.3 ml/min, the smallest inner diameter equaled 95 ± 24.1 µm (Figure 3.11 (B)).

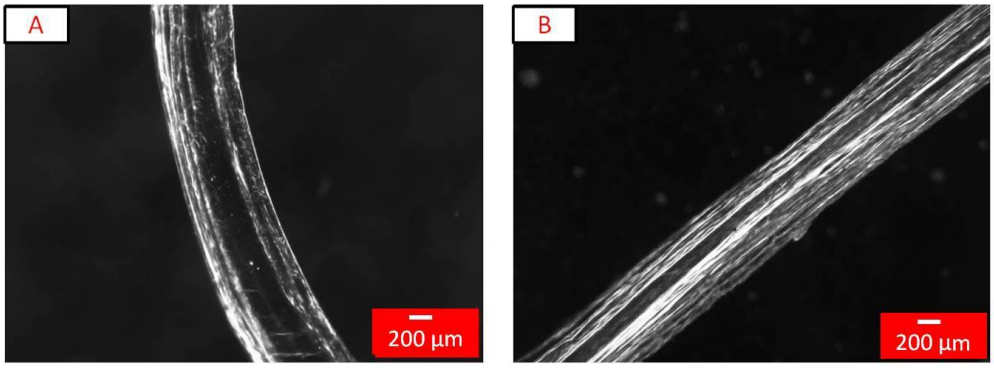

Figure 3.11 (A) The internal diameter of the hollow fiber was largest at the lowest sheath flow rate. (B) The internal diameter of the hollow fiber was smallest at the highest sheath flow rate.

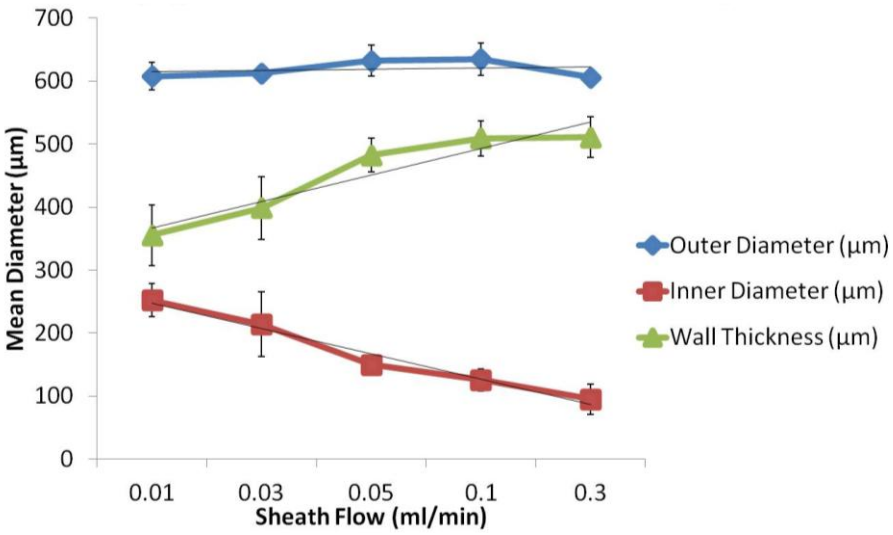

Figure 3.12 At the fixed core flow of 0.5 ml/min, the internal diameters decrease and wall thicknesses increase with increasing sheath flow rates. Bar: SD (n = 3)

As seen in the Figure 3.12, at the fixed core flow 0.50 ml/min, when the sheath flow rates increase, the hollow fibers' wall thicknesses increase and the inner diameters

decrease. The outer diameters did not show any significant change due to increasing of the sheath flow rate.

3.4 Discussion

The dimensions of the alginate microfiber fabricated by the microfluidic device can be adjusted by changing the flow rate without having to re-tool [1]. In this work, we introduced a simple method to generate a continuous hollow microfiber using a PDMS microfluidic device. The main advantages of this technique were that: 1) we could easily control the size of the fibers, 2) the process was simple and rapid, and 3) the method was non-toxic for enzyme immobilization. Alginate solution was introduced as the sheath flow, and $CaCl_2$ solution was introduced as the core flow. The Ca^{2+} ions diffused and crosslinked with sodium alginate to generate the alginate hollow microfibers.

For the microfluidic device using the glass microcapillary, the glass tip was cut using microforge (MF-900, Narishige) equipment [1, 2]. This is an expensive tool with a commercial price of approximately $7,000.00 or greater (source from www.tritechhresearch.com). The PDMS-based microfluidic device can fabricate the microfibers with a simple template platform without any specialized tools. In addition, unlike soft lithography or photolithography, this PDMS microfluidic platform can be fabricated in a wet lab space without cleanroom facilities.

The length of the outlet microchannel was also an important factor for solidification. Similar to another study, the length of the outlet microchannel was 4 cm; this length provides sufficient time for solidification between sodium alginate and Ca^{2+} ions [2]. Using the glass microcapillary-based system, the sheath flow and core flow rates must be kept in a narrow range in order to avoid a spiral curl of the fiber which would subsequently clog the outlet microchannel. In Shin et al. [2] study, they reported that the optimal flow rates used to generate a straight microfiber were 20 ml/h for $CaCl_2$ sheath

flow and 1 μL/min of alginate sample flow rate. Compared to this study, our technique was more efficient because the spiral curl drawback did not occur even at extremely high flow rates. Thus, the range of the flow rate was more flexible than that of the previously mentioned study. For example, the highest flow rate can be increased up to 0.3 ml/min (2% alginate flow rate) and 0.90 ml/min ($CaCl_2$ flow rate). We believed the wide range of flow rate can significantly reduce the time of large scale microfiber fabrication. In our study, the microfluidic device was placed vertically during microfiber generation. This was important to avoid the high surface area contact of the microchannels with the alginate materials because this contact can cause clogging inside PDMS microchannels [2].

The relationship between the flow rates and the microfiber can be explained by the velocity profile [43, 44]. At a fixed sheath flow rate, there was a greater difference in the velocity profile with increasing core flow rate. This result caused the drag force between two fluids to increase and stretch the core flow fluid. On the other hand, the change of flow rate may terminate the Ca^{2+} ion diffusion and affect the residence time of gelation formation [2]. When the sheath flow increased at a constant core flow, the sheath flow focused more, and, hence, the surface area contact between the two fluids increased. Therefore, the Ca^{2+} ion rapidly diffused and crosslinked with alginate pre-polymer.

3.5 Conclusions

The microfluidic device fabrication can be done in a wet lab microenvironment. Unlike previous microstructure fabrications, the hollow microfiber generation via the PDMS-based microfluidic device is straightforward and rapid without requiring high temperature, high pressure, or high voltage. The internal diameter and the wall thickness of alginate hollow microfiber can be controlled by varying flow rates. The advantages of our technique can be carried forward to cell and biocatalyst immobilization; bioreactors,

micro-sensing devices, cell carriers, protein delivery, mimicking blood vessels and cartilage, or bone tissue engineering.

Chapter 4

Enzyme Immobilization and Reactivity in Hollow Alginate Microfiber

4.1 Introduction

Enzyme immobilization has shown great advantages in industries related to biotechnology, food processing, biological detergents, chemical analysis, pharmaceutical and medicine. Enzyme immobilization improves stability in undesirable conditions and prolongs enzyme storage for long periods of time. Although many enzyme immobilization techniques have been shown in many studies, enzyme entrapment is still the most efficient for both industrial and lab settings. Enzyme entrapment locally confines enzymes in a supporting matrix or a membrane. While physical adsorption and covalent crosslink immobilizations require the chemical bonding between immobilized enzymes and supporting substrates, the entrapment allows immobilized enzymes to be free-floating in the confined core spaces of matrices or membranes. In such an immobilized mechanism, the enzyme is retained safely in an undesirable condition without affecting enzyme conformation. In an entrapment method, the supporting material is a critical factor that directly affects the entrapped enzyme efficiency, leaching quantity, and enzyme activity.

Alginate is the most common natural polymer that has been used to immobilize enzymes. Alginate is a linear block copolymer, and its chemical polymerization reaction is not harmful to enzymes. During gelation, the crosslink mechanism of alginate and divalent cations occur spontaneously at the interface surface. Therefore, alginate material can be used as a supporting material without interfering or harming enzyme activity. In addition, alginate natural polymer is biocompatible, biodegradable, non-toxic, and its mechanical strength is controllable. Also, the stability of alginate is independent from temperature; therefore, it is suitable for a wide range of enzymatic immobilizations [11].

The target enzymes can be immobilized by different alginate-based microstructures such as microfiber [32], microbeads/microspheres [45-47], microfilm [48], or microstrips. The previous studies have reported that the low efficiency of immobilized enzymes is mainly due to the large diameters of microbeads/microspheres. In addition, these microstructures contain thin walls, and the immobilized enzymes easily leach or diffuse from the alginate matrix. To overcome these limitations, the microstructures have been coated with additional layers of cationic polymers or nanofilms to increase wall thickness of microbeads/microspheres.

However, the concentration of these cationic polymers must be strictly controlled because they can reduce the entrapped enzyme efficiency and the enzyme activity [45]. For example, in Liu et al. [45] study, the encapsulated enzyme efficiency and the relative activity significantly decreased when coating with an inappropriate concentration of chitosan was done. More importantly, this study indicated that at 3% chitosan coating, the enzyme relative activity was significantly low and it was the same as at 0% chitosan coating (bare microbeads/microspheres). The similar limitation was also reported in Zhu et al. [47] study. The effective enzyme activity decreased when the microspheres were coated with a polyelectrolyte nanofilm. This nanocoating could not prevent the enzyme from leaching out of the support material over time. But, on the other hand, if the coating layers were too thick, it prevented the release of immobilized enzymes from the microbeads. Therefore, we can conclude that it is very difficult to control the diffusion rate of immobilized enzymes using coating layers.

The microstructures may have an effect on efficiency of enzyme immobilization. During alginate microbead gelation, sodium alginate solution was slowly dripped into an aqueous divalent cations solution bath. These microbeads lacked uniformity in size distribution and their gelation rate was hard to control [49]. Compared to a microbead,

the surface area to volume ratio of a continuous hollow microfiber is larger, and the gelation rate is easier to control without the concern of uniformity in microstructure size. In addition, the immobilized enzyme in a microfiber structure is more convenient to continuously monitor [50, 51].

Various methods can produce microfibers such as electrospinning, meltspinning, wetspinning, extrusion, and the use of a microfluidic device. Among these, the microfiber-based microfluidic technique is the most suitable for immobilizing biological sensitive molecules. The microfiber can be fabricated easily without requiring high temperature (meltspinning), high voltage (electrospinning), chemical exposure (wetspinning), or high pressure (extrusion). The available microfluidic device fabrication methods are glass microcapillary-based system, soft lithography, or photolithography. These methods require special tools or a sterile environment (cleanroom facility). In this thesis, a long continuous alginate hollow microfiber was generated using a simple microfluidic device. In addition, the size of the hollow fiber was easily controlled by varying flow rates. This fabricated hollow fiber was then used to immobilize enzymes.

Glucose oxidase (GOx) has been used in various technological applications since the early 1950's [3]. GOx enzyme was purified from different fungi sources such as *Aspergillus* or *Penicillium*. Some applications of GOx are in food and beverage technologies, as an antagonistic component against food-borne pathogens, ingredient of toothpaste, and production of gluconic acid. It is also a main component in biosensors for glucose detection and can estimate the glucose concentration in body fluids [3]. In the presence of oxygen, the GOx enzyme catalyzes the oxidation of β-D-glucose to produce gluconic acid and hydrogen peroxide (H_2O_2). The molecular weight of GOx is in the range of 130-150 kDa [3]. The GOx enzyme only reacts with β-anomer of D-glucose and its activity is inhibited by cations such as Ag^{+}, Hg^{2+} , and Cu^{2+} [3]. The optimum pH of GOx

is in the range of 5.0-7.0 pH [3]. The enzyme stability of the GOx derived from the *Aspergillus* fungi is 40-60 ˚C [3]. GOx enzyme immobilization is widely used in different settings from academic research to industrial applications. Some support materials that can be used for enzyme immobilization are porous glass or cellulose. These materials contain high surface area to volume ratio [3]. The lyophilized GOx enzyme is very stable at -20 $^{\circ}$C for at least 6 months. While the half-life time of GOx can remain about 30 minutes at 37 ˚C, the immobilized GOx enzyme can maintain a more effective half-life at the same temperature [3]. GOx was chosen as a model enzyme in this experiment because it is cost effective, stable, and contains a high purity level [3].

The previous study showed that enzymes were immobilized using an alginate hollow microfiber [32]. The target immobilized enzyme was simply mixed with the alginate solution. The mixture of enzyme and alginate solution then passed through the microfluidic chip and crosslinked with $CaCl_2$ to achieve gelation. However, the side wall of the fabricated microfiber was thin; therefore, the chitosan coating was required to prevent enzyme leaching from the alginate matrix. As reported earlier, the chitosan concentration can interfere with the enzyme encapsulation efficiency and the enzyme activity [45, 47]. Therefore, it is important to minimize the chitosan coating in enzyme immobilization.

The main goal here was to entrap the GOx enzyme in the semi-permeable alginate matrix using a long and continuous alginate hollow microfiber. Based on our knowledge, none of the studies demonstrated the relationship of the parameters of a hollow fiber and the immobilized enzyme activity. Therefore, for the first time, this work clearly demonstrated the effect of wall thickness and the core of the hollow fiber on enzyme entrapment and enzyme activity. Moreover, storage solutions also played an important role in controlling enzyme activity. The concentration of type of metal ions significantly increased or decreased the enzyme activity. Three storage solutions were

investigated in this study: 100 mM $CaCl_2$, 50 mM HEPES buffer solution, and osmotic solution (the mixture of 42 mM NaCl and 15 mM HEPES solution). Our hypotheses were: (1) a hollow fiber with a thick wall and a narrow bore could entrap enzymes with a high efficiency; (2) enzyme activity would be higher in osmotic solution; (3) in a favorable environment, the thick wall and the small core diameter of the alginate microfiber would provide a high surface area to volume ratio; therefore, the biocatalytic conversion would also be high; (4) the thick side wall could act as a barrier to minimize enzyme leaching and to protect the immobilized enzyme in undesirable conditions.

4.2 Materials and Methods

4.2.1 Enzyme Immobilization into the Alginate Hollow Microfiber

The alginate hollow microfiber fabrication was previously described in chapter 3. In brief, the microfluidic device was fabricated using the displaced Y-shaped template method. The inlet and outlet microchannels were approximately 400 μm and 700 μm in diameter. GOx enzyme (lyophilized powder form) was diluted with 50 mM HEPES buffer solution, at a pH of 7.0. To achieve a 2% enzyme-alginate solution, the GOx enzyme solution (1 mg/ml) was mixed with 4% (w/v) alginate solution using a 1:1 ratio. The enzyme-alginate solution was then introduced into the left and right channels while 20 mM $CaCl_2$ was introduced into the main inlet. The hollow microfiber was fabricated with a constant sheath flow rate of 0.05 ml/min and core flow rates of 0.42 ml/min and 0.90 ml/min. The enzyme-load alginate fibers were immersed in 100 mM $CaCl_2$ for 20 minutes to improve the hardness of the fiber. The enzyme-load fibers were then transferred into the following stored solutions: 100 mM $CaCl_2$, HEPES buffer solution (50 mM, pH 7.0), and osmotic solution (the mixture of 42 mM NaCl and 15 mM HEPES buffer solution, at a pH of 7.0). Enzyme activity was measured after 1 hour.

4.2.2 Enzyme Activity after Immobilization

The GOx activity after immobilization was measured as described in the previous studies [51, 52]. The enzyme activity was detected by using the colorimetric method. In brief, the components of the reaction mixture included: 2.4 ml of 0.21 mM *o*-dianisidine solution (diluted with autoclaved DI water, pH 7.4); 0.1 ml of β-D-glucose solution that contained 1 mg/ml in sterilized PBS buffer solution; 0.1 ml of peroxidase solution (1 mg/ml) prepared in sterilized PBS buffer solution. A 4 cm long immobilized fiber was then cut into small pieces and added into the reaction mixture. These contents were gently mixed on the shaker for 45 minutes at room temperature. The brown-orange colored products that resulted from this were then transferred into plastic disposable cuvettes. The enzyme activity was measured using a spectrophotometer at a wavelength absorbance of 500 nm.

The experiment was repeated at least twice; and the average and standard deviation of absorbance of enzyme activity were calculated.

4.3 Results

In general, GOx enzyme catalyzed an oxidation reaction of β-D-glucose in the presence of oxygen (O_2) to produce δ-gluconolactone and hydrogen peroxide (H_2O_2). In the colorimetric assay, *o*-dianisidine dye reacted with H_2O_2 in the presence of peroxidase catalyst to produce oxidized o-dianisidine with an alteration in color:

$$D - Glucose + O_2 + H_2O \xrightarrow{GOx} D - glucono - 1{,}5 - lactone + H_2O_2$$

$$H_2O_2 + o - Dianisidine\ (reduced) \xrightarrow{POD} o - Dianisidine\ (oxidized)$$

(Clear) (Brown)

The oxidized *o*-dianisidine appeared in various colors: yellow, orange, or dark brown. These results indirectly indicated the activity of the GOx enzyme. The absorbance was used to calculate the conservation of immobilized enzyme activity.

As reported in chapter 3, at a constant sheath flow rate, the core diameter decreased; and wall thickness increased with a decrease in core flow rate. Two enzyme-loaded fibers were generated at a fixed sheath flow rate of 0.05 ml/min, and two different core flow rates: 0.42 ml/min and 0.90 ml/min. The generated enzyme-loaded fibers were stored in different storage solutions and the chemical reaction was investigated after 1-2 hours.

After placing the fiber on the shaker for approximately 2-5 minutes, the enzyme activity was indicated by a change in color from clear to an orange-brown color in both samples. However, there was more of a color change of the fiber at a low core flow than at a high core flow (Figure 4.1).

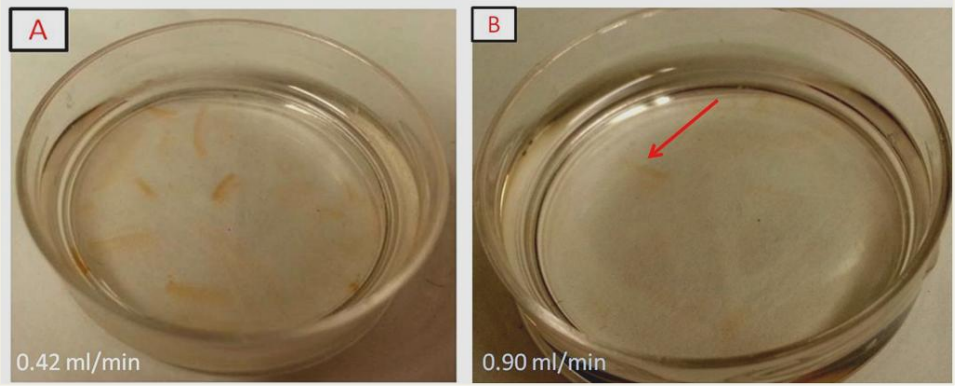

Figure 4.1 The enzyme-loaded fibers are cut and transferred into the reaction mixture. Both fibers are stored in the osmotic solution. The reactions are observed after 2-5 minutes. At the fixed sheath flow, the enzyme reaction is faster and demonstrates more color change in (A) 0.42 ml/min than (B) 0.90 ml/min.

The reaction was completed after 45 minutes. The colored products were transferred into cuvettes. As indicated in Figure 4.2, the immoblized enzyme activity in a hollow fiber with a small core diameter was cleary different from the one with a large core diameter. At the core flow rate of 0.42 ml/min, the products of the reactions were darker and more brownish in color than the products of immobilized enzymes with a higher core flow rate.

The enzyme activities were also different in the various storage solutions. In 100 mM $CaCl_2$ solution, the products of both core flow rates appeared to be light yellow. In osmotic solution, the final products portrayed a dark brown color. The different colors of products were directly related to the quantity and activity of the immobilized enzymes.

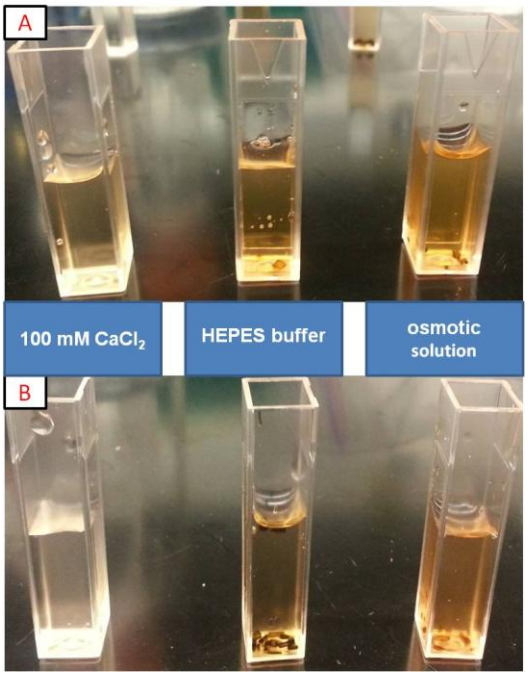

Figure 4.2 The enzyme activity completed after 45 minutes. The enzyme activities are different in the various storage solutions: (A) 0.42 ml/min and (B) 0.90 ml/m.

At a fixed sheath flow of 0.05 ml/min, the varying core flow rate caused a change in the internal diameter and the wall thickness. At 0.42 ml/min, the internal diameter was approximately 134 ± 2.75 µm and the wall thickness was 507 ± 30.29 µm. In contrast, at 0.90 ml/min, the internal diameter of the hollow fiber was 278 ± 78.83 µm and the wall thickness equaled 380 ± 45.62 µm. As shown in Figure 4.3, the immobilized enzyme stability and activity was higher in the microfiber that contained a small internal diameter with a thick side wall. In an unfavorable condition of 100 mM $CaCl_2$ as a storage solution, the immobilized enzyme activity in a microfiber with a small internal diameter was significantly high compared to the enzyme activity of a microfiber with a large internal diameter. This can be explained by the thick side wall effectively protecting the immobilized enzyme in an undesirable condition.

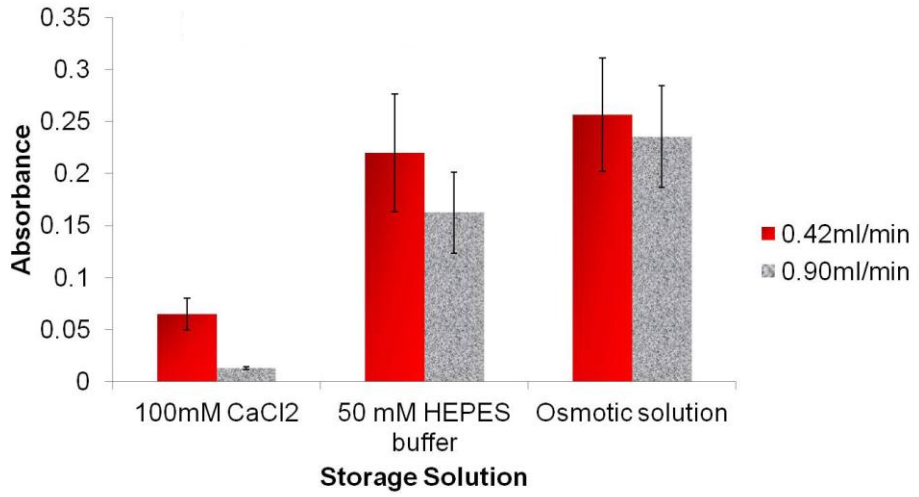

Figure 4.3 The effect of core flow rates and the storage solutions on the activity of the GOx enzyme.

As shown in Figure 4.3, the immobilized enzyme activity also depended on the storage solution. The enzyme activity was highest in the osmotic solution which

contained 42 mM NaCl and 15 mM HEPES, pH 7.0. However, in 100 mM $CaCl_2$ storage solution, the enzyme activity was significantly low. As expected, in the HEPES buffer solution the enzyme activity was higher than in the 100 mM $CaCl_2$ solution.

4.4 Discussion

In this work, we investigated the effect of microfiber dimensions on the quantity and activity of the immobilized enzyme. The GOx enzyme was immobilized via the entrapment method that confined the enzyme molecules into a semi-permeable alginate matrix. The surface area of alginate matrix was a critical factor in the efficiency of immobilized enzymes. With a thicker wall, it provided more surface area for entrapping enzymes. On the other hand, when the core diameter of hollow fiber decreased, the reaction was faster because of a higher surface area to volume ratio. The substrate rapidly penetrated and stimulated the oxidized reaction. In addition, the thick side wall acted as a barrier to maintain the stability of the enzyme in an undesirable condition. It also prevented enzymes from leaching out of the alginate matrix.

The storage solutions also played important roles in the immobilized enzyme activity. In 100 mM $CaCl_2$ solution, the activity of GOx was significantly low compared to other storage solutions. The result was similar to those reported before [53]. The metal ions in a high salt concentration acted as inhibitors that reduced the enzyme activity. To perform its function as a catalyst, GOx needed the presence of cofactor flavin adenine dinucleotide (FAD) to perform in the oxidation-reduction reaction. In a high salt concentration, such as 100 mM $CaCl_2$ solution, the presence of numerous metal ions competed with FAD for a binding site at an active site of GOx. This action interfered with the hydrogen bonding of FAD and pyrophosphate or ribose group at the enzyme active site. In addition, the presence of a large number of metal ions also competed with

enzyme substrates for the binding site on an active center. This partially inhibited the activity of enzymes [53].

In the osmotic solution, the enzyme activity proved to be the most efficient among the three storage solutions. It indicated that the quantity of the GOx immobilized enzyme on the wall of the hollow fiber was stable, and the enzymatic activity was the highest. The effects of divalent and monovalent cations on enzyme activity are different. At an enzyme active site, the divalent cations attach to pyrophosphate with a much stronger handhold than the monovalent cations. Therefore, the enzymatic inhibition that was caused by the binding of the divalent ions was also greater than the monovalent ions [53]. Here, the enzyme activity was affected by the presence of Ca^{2+} ions from $CaCl_2$ solution and Na^+ from the osmotic solution. The metal ions can act as either activation or inhibition activity in the GOx enzyme. In 42 mM NaCl, Na^+ ions maintained the stability of enzyme conformation and transformed it into an active form with an appropriate change. This result subsequently led to higher enzyme activity [53]. The enzyme activity in the osmotic solution was higher in HEPES buffer solution because of the presence of Na^+ ions.

The limitation in this study was the requirement to expose the generated fiber to 100 mM $CaCl_2$ solution at least 20 minutes before transferring it to the storage solutions. This step was necessary to improve the hardness of the microfiber, but it could potentially reduce the enzyme activity.

4.5 Conclusions

The experiments demonstrated that an alginate hollow microfiber with a narrow core diameter and a thick side wall improved enzyme immobilization. The thick wall of the hollow fiber not only increased the surface area for enzyme immobilization, but it also acted as a barrier that prevented enzymes from leaching out of the alginate matrix. The

immobilized enzyme activity was investigated after immobilization by using the colorimetric protein assay. This showed that the presence of metal ions in the storage solution could either inhibit or be the activation factor for the enzyme activity. Based on our results, the enzyme-loaded alginate hollow microfiber can be a model for studies in chemical synthesis, biotransformation, biomolecular reaction, or glucose detection.

Chapter 5

Future Works

5.1 Long Term Enzyme Stability

Based on the results in chapter 4, the alginate hollow microfiber provides a suitable biological environment for immobilizing GOx. The thick wall of the hollow fiber prevents the enzyme leakage and maintains the stability of the immobilized enzyme. The GOx-loaded hollow fiber can be widely used as a chemical sensor that can monitor chemical processes or biological systems. In the current work, the enzyme activity was stable and efficient, and the whole process was simple and cost effective. Working on these lines, the next step can be to maintain the enzyme activity for a longer period of time so the immobilized enzyme is reusable and the process can be scaled to an industrial high-throughput setting.

Several critical factors would contribute to the successful immobilization of enzymes for prolonged periods of time. First, the efficiency of the immobilized enzyme depends on the diameter of the core space and the thickness of the alginate fiber wall. The optimal core diameter and wall thickness of microfiber can be achieved by controlling core and sheath flow rates. Other parameters, such as the angle of branched channels and their effect on the outer diameter, core diameter, or wall thickness, have not yet been tested and defined. Therefore, future studies can focus on the analysis of microfluidic devices with different angular spacing between them. Second, the stability and activity of an immobilized enzyme for long term reusability depends on the storage solution and storage conditions. The storage solutions not only affect enzyme stability, but they can also cause physical changes in the supporting materials. For example, the storage solution containing MES buffer can cause the alginate fiber to swell after 24 hours (Figure

5.1), or the phosphate buffer solution at pH 7.0 can dissolve the alginate fiber in only 10-15 minutes.

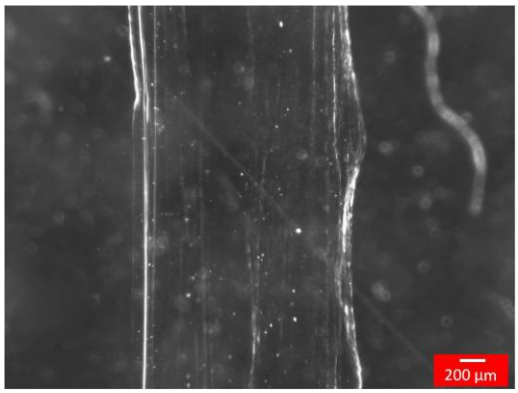

Figure 5.1 The hollow alginate microfiber swollen in MES buffer solution after 24 hours. The physical shape of the alginate microfiber is also changed.

The type of storage solutions, appropriate pH, salt concentrations, and presence of metal ions are all important factors for prolonged enzyme immobilization and stability.

5.2 Modify Microfluidic Device Using Template Methods

In this study, a single long fiber with a single core space was uniformly generated from one end to the other. In future, this device can be modified to fabricate a long single hollow fiber with multiple core spaces.

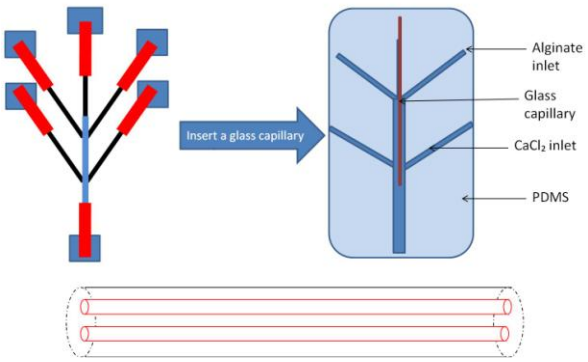

Figure 5.2 The modified device can generate a long single fiber with two core spaces.

Using a modified microfluidic device similar to the one indicated in Figure 5.2 and the double-coaxial laminar flow mechanism, a single, long, dual inner core fiber with an outer tubular microstructure can be fabricated. With this multiple core fiber microstructure, multiple biocatalyst components could potentially be immobilized in a single hollow microfiber. Moreover, the double side wall of microfiber can increase the efficiency of the immobilized enzyme. Besides that, such microfiber structure can be very useful for the study of multiple chemical reactions that strictly depend on precise time control.

5.3 Implantable Biosensor for Continuously Monitoring Glucose Concentration

The free GOx enzyme activity is different between *in vitro* and *in vivo*. As demonstrated in Valdes et al. [54], the activity of GOx slightly decreased in the presence of glucose *in vitro*. However, *in vivo*, the presence of glucose caused a rapid reduction of GOx enzyme activity that was lower than in vitro because of production of H_2O_2. Therefore, to use GOx as a glucose biosensor, it must be immobilized to improve its stability.

Although GOx has been applied widely in different industries, the use of enzyme immobilization in the continuous glucose monitoring system is still a new technological innovation. The biosensor that uses a fibrous microstructure is more suitable for continuously monitoring than using an enzyme electrode [55]. The enzyme electrodes have been used for over decades to monitor glucose concentration in blood in vivo [50]. However, the limitations of this technique are: (1) instability after implantation, (2) inaccurate measurements of low blood glucose concentrations, and (3) short-term functionality [50]. In addition, the glucose monitor that uses an enzyme electrode cannot continuously monitor blood glucose concentration [56]. Recently, hydrogel-based microbeads have been used in vivo to replace the enzyme electrodes for glucose

detection. These hydrogel-based microbeads are easy to inject into the body via a non-invasive method, and it does not cause any inflammation to the host body [57]. For long-term monitoring, the hydrogel-based biosensor device has to function for a long period of time and be easily removed without an invasive procedure. However, hydrogel-based microbeads do not meet all of the requirements. The hydrogel-based microbeads are not stable at the implant site and spread widely and randomly from the local site. More importantly, it is not easy to remove the microbeads from the implanted site [50].

The microfiber-based sensor is a promising field for continuously controlling and monitoring glucose in vitro and in vivo. The fiber-based sensor can work as an individual sensor or as a part of a sensor device. Recently, the aim of this fiber-based sensor is to function over long periods of time in vivo to prevent the need to frequently replace the biosensor. For long-term monitoring the fiber-based sensor has several advantages over the microbeads structure, namely: (1) steady at the implanted site for long-term; (2) ease in controlling specific length or size of the biosensor to avoid invasive rupture at the implant site; (3) ease in removing from the body non-invasively [50]. Compared to the microbeads structure, the contact area between the fiber and the implanted tissue increases which leads to a decrease in mobility [50]. In previous studies, the blood glucose concentration has been monitored continuously by fluorescent or optical microfiber-based sensors. However, *in vivo*, the host inflammatory response still remains as essential drawback due to the lack of biocompatibility of the hydrogel polymer.

As we know, alginate is a natural biopolymer that is biocompatible and biodegradable; therefore, inflammation or immune response of the host body at a fiber-tissue interface can be minimized without having to use an anti-inflammatory agent. While the implanted fiber sensor in the previous study was 1000 μm in diameter [50], our microfiber had a smaller diameter which can minimize the damage of the tissue at an

implanted site. In addition, a smaller fiber diameter contains a higher surface area to volume ratio which has a faster response rate [50]. Instead of using the synthetic fluorescent hydrogel, the GOx can be distributed with other fluorescent components such as fluorescein derivative-GOx enzyme via covalent bond [56] or “FITC-conjugated dextran” [58].

References

1. Jeong, W., et al., *Hydrodynamic microfabrication via "on the fly"• photopolymerization of microscale fibers and tubes.* Lab on a Chip, 2004. **4**(6): p. 576-580.
2. Shin, S.-J., et al., *"On the fly" continuous generation of alginate fibers using a microfluidic device.* Langmuir, 2007. **23**(17): p. 9104-9108.
3. Bankar, S.B., et al., *Glucose oxidase-an overview.* Biotechnology advances, 2009. **27**(4): p. 489-501.
4. Tischer, W. and F. Wedekind, *Immobilized enzymes: methods and applications*, in *Biocatalysis-from discovery to application*. 1999, Springer. p. 95-126.
5. Spahn, C. and S.D. Minteer, *Enzyme immobilization in biotechnology.* Recent patents on Engineering, 2008. **2**(3): p. 195-200.
6. Gorecka, E. and M. Jastrzebska, *Immobilization techniques and biopolymer carriers.* Biotechnology and Food Science, 2011: p. 65.
7. Datta, S., L.R. Christena, and Y.R.S. Rajaram, *Enzyme immobilization: an overview on techniques and support materials.* 3 Biotech, 2013. **3**(1): p. 1-9.
8. Gunatillake, P.A. and R. Adhikari, *Biodegradable synthetic polymers for tissue engineering.* Eur Cell Mater, 2003. **5**(1): p. 1-16.
9. Lee, K.Y. and D.J. Mooney, *Alginate: properties and biomedical applications.* Progress in polymer science, 2012. **37**(1): p. 106-126.
10. Draget, K.I., G.O. Phillips, and P.A. Williams, *Alginates.* Handbook of hydrocolloids, 2009: p. 807-828.
11. Draget, K.I. and C. Taylor, *Chemical, physical and biological properties of alginates and their biomedical implications.* Food Hydrocolloids, 2011. **25**(2): p. 251-256.
12. Otterlei, M., et al., *Induction of cytokine production from human monocytes stimulated with alginate.* Journal of immunotherapy, 1991. **10**(4): p. 286-291.
13. Soon-Shiong, P., et al. *An immunologic basis for the fibrotic reaction to implanted microcapsules*. in *Transplantation proceedings*. 1991.
14. Espevik, T., et al., *The involvement of CD14 in stimulation of cytokine production by uronic acid polymers.* European journal of immunology, 1993. **23**(1): p. 255-261.
15. Otterlei, M., et al., *Similar mechanisms of action of defined polysaccharides and lipopolysaccharides: characterization of binding and tumor necrosis factor alpha induction.* Infection and immunity, 1993. **61**(5): p. 1917-1925.
16. Klock, G., et al., *Biocompatibility of mannuronic acid-rich alginates.* Biomaterials, 1997. **18**(10): p. 707-713.
17. Turner, T.D., O. Spyratou, and R.J. Schmidt, *Biocompatibility of wound management products: Standardization of and determination of cell growth rate in L929 fibroblast cultures.* Journal of pharmacy and pharmacology, 1989. **41**(11): p. 775-780.
18. Bouhadir, K.H., et al., *Degradation of partially oxidized alginate and its potential application for tissue engineering.* Biotechnology progress, 2001. **17**(5): p. 945-950.
19. Morch, Y.A., et al., *Effect of Ca^{2+}, Ba^{2+}, and Sr^{2+} on alginate microbeads.* Biomacromolecules, 2006. **7**(5): p. 1471-1480.
20. Drury, J.L., R.G. Dennis, and D.J. Mooney, *The tensile properties of alginate hydrogels.* Biomaterials, 2004. **25**(16): p. 3187-3199.

21. Eiselt, P., K.Y. Lee, and D.J. Mooney, *Rigidity of two-component hydrogels prepared from alginate and poly (ethylene glycol)-diamines.* Macromolecules, 1999. **32**(17): p. 5561-5566.
22. Lee, K.Y., K.H. Bouhadir, and D.J. Mooney, *Controlled degradation of hydrogels using multi-functional cross-linking molecules.* Biomaterials, 2004. **25**(13): p. 2461-2466.
23. Zhao S, C.M., Li H, Li L, Xu W., *Synthesis and characterization of thermo-sensitive semi-IPN hydrogels based on poly(ethylene glycol)-co-poly(epsilon-caprolactone) macromer, N-isopropylacrylamide, and sodium alginate.* Carbohydr Res. , 2010. **345**(3): p. 425-31.
24. Maiti, S., et al., *Adipic acid dihydrazide treated partially oxidized alginate beads for sustained oral delivery of flurbiprofen.* Pharmaceutical Development and Technology, 2009. **14**(5): p. 461-470.
25. Bouhadir, K.H., E. Alsberg, and D.J. Mooney, *Hydrogels for combination delivery of antineoplastic agents.* Biomaterials, 2001. **22**(19): p. 2625-2633.
26. Lucinda-Silva, R.M., H.r.R.N. Salgado, and R.C. Evangelista, *Alginate-chitosan systems: In vitro controlled release of triamcinolone and in vivo gastrointestinal transit.* Carbohydrate Polymers, 2010. **81**(2): p. 260-268.
27. Silva, C.M., et al., *Insulin encapsulation in reinforced alginate microspheres prepared by internal gelation.* european journal of pharmaceutical sciences, 2006. **29**(2): p. 148-159.
28. Lee, J. and K.Y. Lee, *Injectable microsphere/hydrogel combination systems for localized protein delivery.* Macromolecular bioscience, 2009. **9**(7): p. 671-676.
29. Tamayol, A., et al., *Fiber-Based Tissue Engineering: Progress, Challenges, and Opportunities.* Biotechnology advances, 2012.
30. Teo, W.E. and S. Ramakrishna, *A review on electrospinning design and nanofibre assemblies.* Nanotechnology, 2006. **17**(14): p. R89.
31. Hwang, C.M., et al., *Controlled cellular orientation on PLGA microfibers with defined diameters.* Biomedical microdevices, 2009. **11**(4): p. 739-746.
32. Asthana, A., et al., *Bromo-oxidation reaction in enzyme-entrapped alginate hollow microfibers.* Biomicrofluidics, 2011. **5**: p. 024117.
33. Mazzitelli, S., et al., *Optimised production of multifunctional microfibres by microfluidic chip technology for tissue engineering applications.* Lab on a Chip, 2011. **11**(10): p. 1776-1785.
34. Yamada, M., et al., *Microfluidic synthesis of chemically and physically anisotropic hydrogel microfibers for guided cell growth and networking.* Soft Matter, 2012. **8**(11): p. 3122-3130.
35. Mata, A., A.J. Fleischman, and S. Roy, *Characterization of polydimethylsiloxane (PDMS) properties for biomedical micro/nanosystems.* Biomedical microdevices, 2005. **7**(4): p. 281-293.
36. Jeong, W.J., et al., *Continuous fabrication of biocatalyst immobilized microparticles using photopolymerization and immiscible liquids in microfluidic systems.* Langmuir, 2005. **21**(9): p. 3738-3741.
37. Kang, E., et al., *Novel PDMS cylindrical channels that generate coaxial flow, and application to fabrication of microfibers and particles.* Lab on a Chip, 2010. **10**(14): p. 1856-1861.
38. Choi, C.-H., et al., *Microfluidic fabrication of complex-shaped microfibers by liquid template-aided multiphase microflow.* Lab on a Chip, 2011. **11**(8): p. 1477-1483.
39. Hwang, C.M., et al., *Microfluidic chip-based fabrication of PLGA microfiber scaffolds for tissue engineering.* Langmuir, 2008. **24**(13): p. 6845-6851.

40. Matteson, M. and C. Orr, *Filtration: principles and practices*. Vol. 27. 1987: CRC Press.
41. Belitz, H.-D., W. Grosch, and P. Schieberle, *Food Chemistry*. 4th revised and extended edition ed. 2009: Springer.
42. Rajput, R.K., *A textbook of fluid mechanics*. 2008: S. Chand.
43. Sakai, S., et al., *Horseradish peroxidase/catalase-mediated cell-laden alginate-based hydrogel tube production in two-phase coaxial flow of aqueous solutions for filament-like tissues fabrication.* Biofabrication, 2013. **5**(1): p. 015012.
44. Takei, T., et al., *Development of mammalian cell-enclosing calcium-alginate hydrogel fibers in a co-flowing stream.* Biotechnology journal, 2006. **1**(9): p. 1014-1017.
45. Liu, Q., A.M. Rauth, and X.Y. Wu, *Immobilization and bioactivity of glucose oxidase in hydrogel microspheres formulated by an emulsification-internal gelation-adsorption-polyelectrolyte coating method.* International journal of pharmaceutics, 2007. **339**(1): p. 148-156.
46. Wang, X., K.-X. Zhu, and H.-M. Zhou, *Immobilization of glucose oxidase in alginate-chitosan microcapsules.* International journal of molecular sciences, 2011. **12**(5): p. 3042-3054.
47. Zhu, H., et al., *Combined physical and chemical immobilization of glucose oxidase in alginate microspheres improves stability of encapsulation and activity.* Bioconjugate chemistry, 2005. **16**(6): p. 1451-1458.
48. Blandino, A., M. Macias, and D. Cantero, *Immobilization of glucose oxidase within calcium alginate gel capsules.* Process Biochemistry, 2001. **36**(7): p. 601-606.
49. Kuo, C.K. and P.X. Ma, *Ionically crosslinked alginate hydrogels as scaffolds for tissue engineering: part 1. Structure, gelation rate and mechanical properties.* Biomaterials, 2001. **22**(6): p. 511-521.
50. Heo, Y.J., et al., *Long-term in vivo glucose monitoring using fluorescent hydrogel fibers.* Proceedings of the National Academy of Sciences, 2011. **108**(33): p. 13399-13403.
51. Deep, A., et al., *Immobilization of enzyme on long period grating fibers for sensitive glucose detection.* Biosensors & bioelectronics, 2012. **33**(1): p. 190.
52. Lee, Y., et al., *Micropatterned assembly of silica nanoparticles for a protein microarray with enhanced detection sensitivity.* Biomedical microdevices, 2010. **12**(3): p. 457-464.
53. Lu, T., et al., *The production of glucose oxidase using the waste myceliums of Aspergillus niger and the effects of metal ions on the activity of glucose oxidase.* Enzyme and microbial technology, 1996. **19**(5): p. 339-342.
54. Valdes, T.I. and F. Moussy, *In vitro and in vivo degradation of glucose oxidase enzyme used for an implantable glucose biosensor.* Diabetes Technology & Therapeutics, 2000. **2**(3): p. 367-376.
55. Monk, D.J. and D.R. Walt, *Optical fiber-based biosensors.* Analytical and bioanalytical chemistry, 2004. **379**(7-8): p. 931-945.
56. Heo, Y.J. and S. Takeuchi, *Towards Smart Tattoos: Implantable Biosensors for Continuous Glucose Monitoring.* Advanced healthcare materials, 2013. **2**(1): p. 43-56.
57. Shibata, H., et al., *Injectable hydrogel microbeads for fluorescence-based in vivo continuous glucose monitoring.* Proceedings of the National Academy of Sciences, 2010. **107**(42): p. 17894-17898.

58. Chaudhary, A. and R. Srivastava, *Glucose sensing using competitive binding assay co-encapsulated in uniform sized alginate microspheres.* Sensor Letters, 2008. **6**(2): p. 253-260.

Biographical Information

Uyen H. T. Pham was born in Vietnam. She moved to United State in 2002 and joined University of Texas at Arlington in 2007 as a pre-medical student. In 2009, she continued in the five-year program to pursue Master of Science in Bioengineering program.

Dr. Samir M. Iqbal offered her a chance to join his lab in November 2009 and to work as a research assistant in the Nano-Bio Laboratory. Throughout these years, she has been involved in several projects such as chemical synthesis of nano/micro fibers, enzyme immobilization, validation of cancer detection on aptamer based nano-textured chips, non-lithographic PDMS microchannel fabrication, and CMOS chip based DNA detection.